Cardioprotective effect of poly(ADP-ribose)polymerase inhibition

PhD thesis

Author: Eva Bartha M.D.

Program leader: Prof. Kalman Toth M.D., Ph.D., Sc.D.
Project leader: Robert Halmosi M.D., Ph.D.

First Department of Medicine
University of Pécs, Medical School
Hungary

2010.

Contents:

1. Abbrevations

AIF	apoptosis-inducing factor
BNP	B-type natriuretic peptide
BW	body weight
CFY	CFY Sprague-Dawley rat
DAP	diastolic arterial blood pressure
EF	ejection fraction
ERK 1/2	extracellular signal-regulated kinase
FS	fractional shortening
GSK-3β	glycogen synthase kinase-3β
HF	heart failure
IR	ischemia-reperfusion
ISO	isoproterenol hydrochloride
IVS (d)	thickness of interventricular septum in diastole
IVS (s)	thickness of interventricular septum in systole
JNK	c-jun N-terminal kinase
LVEDV	left ventricular end-diastolic volume
LVESV	left ventricular end-systolic volume
LVID (d)	left ventricular end-diastolic diameter
LVID (s)	left ventricular end-systolic diameter
MAP	mean arterial blood pressure
MAPK	mitogen activated protein kinase
MTT	3-[4,5-dimethylthiazol-2-yl]-2,5-diphenyltetrazolium bromide
NAD^+	nicotinamide adenine dinucleotide
NIH	National Institute of Health
NOS	nitric oxide synthase
PAR	poly(ADP-ribose)polymers
PARP	poly(ADP-ribose)polymerase
PI3K	phosphatidylinositol-3-kinase
PKC	protein kinase C

PW (d)	thickness of left ventricular posterior wall in diastole
PW (s)	thickness of left ventricular posterior wall in systole
PTP	permeability transition pore
ROS	reactive oxygen species
RWT	relative wall thickness
SAP	systolic arterial pressure
SEM	standard error of the mean
SHR	spontaneously hypertensive rat
TBS	TRIS-buffered saline
TL	lenght of right tibia
WV	weight of ventricles

2. Background:

2.1. Effect of free radicals and poly(ADP-ribose)polymerase (PARP) enzyme inhibition on the heart and the mitochondria

Accumulating evidences suggest that reactive oxygen and nitrogen species are generated in cardiomyocytes and endothelial cells during myocardial ischemia/reperfusion injury (IR), various forms of heart failure (HF) or cardiomyopathies, circulatory shock, cardiovascular aging, diabetic complications, myocardial hypertrophy, atherosclerosis, and vascular remodelling following injury (1, 2).

Reactive oxygen species (ROS) are produced in the ischemic myocardium especially during and after reperfusion when electron transport resumes in the mitochondria after suppression by ischemia (58, 59). ROS are generated secondarily from nicotinamide adenine dinucleotid phosphate (NADPH) oxidases in vascular cells and myocytes, as well as from neutrophils infiltrating the sites of injury. ROS are also generated as a by-product of ATP catabolism; xanthine oxidase and hypoxanthine levels increase during ischemia, and superoxide is produced when hypoxanthine is oxidized to xanthine by xanthine oxidase and again when xanthine is further oxidized to urate. In the vasculature, ROS interact with nitrogen monoxide (NO), generating the highly reactive peroxinitrite ($ONOO^-$) radical, with the dual effect of decreasing the bioavailability of NO, causing vasoconstriction, and aggravating oxidative damage (58).

These reactive species induce oxidative DNA damage and consequent activation of the PARP. The nuclear enzyme PARP-1 is the most abundant isoform of the PARP enzyme family (2,4). PARP-1 functions as a DNA damage sensor and signaling molecule binding to both single- and double-stranded DNA breaks. Upon binding to damaged DNA, PARP-1 forms homodimers and catalyzes the cleavage of nicotinamide adenine dinucleotide (NAD^+) into nicotinamide and ADP-ribose to form long branches of ADP-ribose polymers on glutamic acid residues of a number of target proteins including histones and PARP-1 (automodification domain) itself. Poly(ADP-ribosylation) deliberates negative charge to histones leading to electrostatic repulsion among histones and DNA, a process implicated in chromatin remodeling, DNA repair, and transcriptional

regulation. Numerous transcription factors, DNA replications factors, and signaling molecules have also been shown to become poly(ADP-ribosylated) by PARP-1. The effect of PARP-1 on the function of these proteins is achieved by noncovalent protein-protein interactions or by covalent poly(ADP-ribosylation) (1).

Reactive oxygen and nitrogen species (e. g., peroxynitrite)-dependent citotoxicity in various cardiovascular diseases is mediated by a multitude of effects including lipid peroxidation, protein nitration and oxidation, DNA oxidative damage, activation of matrix metalloproteinases, and inactivation of a series of enzymes. Mitochondria are not only the source of initiating ROS but also are the focal sensors that translate the redox stress signal into a cellular-death response (58). Mitochondrial enzymes are particularly vulnerable to attacks by peroxynitrite, leading to reduced ATP formation and induction of mitochondrial permeability transition pore (PTP) opening, which dissipates the mitochondrial membrane potencial (1, 5). The mitochondrial PTP is a non-selective large conductance channel in the mitochondrial inner membrane, which is physiologically closed. Opening of mitochondrial PTPs is involved in cell death induced by a variety of causes (for example, IR, alcohol, endotoxin, anti-cancer agents) (57). The above mentioned events lead to cessation of electron transport and ATP formation, mitochondrial swelling, and permeabilization of the outer mitochondrial membrane (intrinsic pathway: regulated by the members of the Bcl-2 family), allowing flux of several proapoptotic molecules, including cytochrome C and apoptosis-inducing factor (AIF) (59, 61). The members of Bcl-2 family proteins can antagonize the activity of prosurvival proteins, stimulate prodeath proteins, and promote apoptosis. Growth and survival factors inhibit the death promoting activity of Bad (BH3-only protein, member of the Bcl-2 family) by stimulating phosporylation at multiple sites. Phosphorylation of Bad by the Akt kinase at Ser-136 is an important point of cross-talk between survival kinase and death pathway leading to protection of the heart against ischemic injury (58).

In turn, cytochrome C and AIF activate a series of downstream effectors, which eventually results in the fragmentation of nuclear DNA (1, 5). Studies using radio-labelled 2-deoxyglucose as a tracer of opened mitochondrial PTPs indicated that mitochondrial PTPs open within 5-10 min after reperfusion but not during ischemia. Because molecules smaller than 1.5 kDa pass through mitochondrial PTPs, irreversible

PTP opening abolishes mitochondrial membrane potential, disabling the mitochondria to produce ATP (58).

In addition to its damaging effects on mitochondria, peroxynitrite inflicts more or less severe oxidative injury to DNA, resulting in DNA strand breakage, which in turn activates the nuclear enzyme PARP. Activated PARP consumes NAD to build up poly(ADP-ribose)polymers (PAR). Some free PAR may exit the nucleus and travel to mitochondria, where they amplify the mitochondrial efflux of AIF (nuclear to mitochondria crosstalk). Depending on the severity of the initial insult by peroxynitrite or other oxidants, the injured cell may either recover or die. In the latter case, the cell may be executed by apoptosis in the case of moderate PTP opening and PARP activation with preservation of cellular ATP, or by necrosis in case of widespread PTP opening and PARP overactivation, leading to massive NAD consumption and collapse of cellular ATP (1, 5).

There are oxidant sources in the heart, altough the impact of their inhibition on hypertrophic remodeling remains unclear. Myocardial reactive oxygen species (ROS) sources include xanthine and NADPH oxidases, mitochondrial electron transport, and nitric oxide synthase (NOS), the cyclooxygenase pathway of arachidonic acid metabolism and the respiratory burst of phagocytic cells (3, 6). Among these, some recent evidence suggest that NOS may be particularly important to more advanced dilatative diseases. Xanthine oxidase-derived free radicals have been found to play a role in dilated cardiac failure, and allopurinol and its active metabolite, oxypurinol, which block xanthine oxidase, also improve myocardial efficiency, NO-ROS balance. However, in clinical trials, these drugs did not improve symptoms or exercise capacity. ROS leakage linked to mitochondrial electron transport may also contribute to heart failure (3). In the heart, ROS can evoke cytotoxicity, myocardial stunning, arrythmia, reduction of the calcium transient and contractility, elevated diastolic calcium levels and intracellular ATP depletion (6).

2.2. Intracellular signaling pathways and oxidative stress

A number of physiological, pharmacological and pathological stimuli initiate cardiac hypertrophy (7). In addition, cardiac hypertrophy is associated with alterations in intracellular signaling transduction pathways, including alterations of G-protein-coupled receptors, small G protein, mitogen activated protein kinase (MAPK), protein kinase C (PKC), calcineurin and calmodulin and so on. Various signaling pathways are involved in the complicated interactions that finally promote cardiac hypertrophy and HF (8).

Growing evidences suggest that normal cardiac growth and exercise-induced hypertrophy are in large part regulated by the PI3K/Akt pathway. Many pro-hypertrophic stimuli have been shown to activate the serine/threonine kinase Akt, and PI3K-activation is an important common step in this process. Of the 3 Akt genes, only Akt-1 and -2 are expressed at substantial levels in the heart (9). Akt has two downstream targets: mammalian target of Rapamycin (mTOR) and Glycogen synthase kinase 3β (GSK-3β) (5, 6). Recent studies revealed an important role for Akt-signaling in cardiac angiogenesis. Ineffective angiogenesis might contribute to the transition from hypertrophy to HF (9). The activity of GSK-3β is controlled by the phosphorylation status of serine-9. Several protein kinases, including Akt, inactivate GSK-3 β by phosphorylation of serine-9 (5, 6, 9).

Growing data suggest that modulation of the complex network of MAPK cascades could be a rewarding approach to treat cardiomyocyte hypertrophy and HF (7, 9). The MAPKs are elements of three-tiered protein kinase cascades and comprise basically three subfamilies, the extracellular signal-regulated kinases (ERKs), c-jun N-terminal kinases (JNKs) and the p38 MAPKs. While the ERKs are particularly implicated in growth-associated responses, the latter two groups are generally activated by cytotoxic stress factors (9).

Protein kinase C (PKC) is critically involved in the development of cardiac hypertrophy and HF. Furthermore, the data also suggest that individual PKC isoforms have different effects on signaling pathways, variously leading to changes in cardiac contractility, hypertrophic response, and tolerance to myocardial ischemia in the heart (8).

Several studies suggest that PARP inhibitors can modulate these intracellular signaling pathways beneficially in various forms of HF or cardiomyopathies, circulatory shock, cardiovascular aging, diabetic complications, myocardial hypertrophy, atherosclerosis, vascular remodeling following injury and during myocardial IR (1, 2, 5, 6,).

2.3. Experimental models of cardiac oxidative injury

To reveal the effect of PARP inhibitors on intracellular signaling pathways and echocardiographic parameters in rats, two experimental models were used. First, we investigated the action of PARP inhibition in vivo in a postinfarction herat failure model, then PARP inhibitor agent was tested in a hypertensive heart failure model.

Subcutaneous administration of the beta-adrenoreceptor agonist isoproterenol induces extensive amount of cardiomyocyte necrosis, ranging from patchy subendocardial necrosis to transmural infarction, while patency of coronary vasculature is maintained (10, 11, 12). Cardiac remodeling is seen in isoproterenol infused rats with severe myocardial hypertrophy accompanied by myocardial injury, and beta-adrenoreceptor-mediated apoptosis has also been demonstrated in cardiomyocytes (11). It has been also demonstrated that isoproterenol administration produces free radicals via beta-adrenoreceptor mechanism that affects the cell metabolism to such degree that cytotoxic free radicals are formed producing myocardial necrosis (12). Increased oxidative stress resulting from an increased cardiac generation of ROS is implicated in the progression of cardiac hypertrophy and HF (11).

SHR have been widely used as a model for hypertensive heart disease (13). The SHR was originally introduced by Okamoto and Aoki as a model of genetic hypertension. The progression from hypertrophy to impaired cardiac function in the SHR is similar to the clinical course of patients with hypertension. Persistent hypertension develops in the SHR after approximately 6 weeks of age. Following a relatively long period of stable hypertension and compensated hypertrophy, at approximately 18 months of age, animals begin to develop evidence of impaired function (tachypnea, labored respiration). After the age of 18 months, mortality rate is increased, pathologic features suggesting HF; e.g effusions, left atrial thrombi and right ventricular hypertrophy. Findings in these animals

are consistent with observation of cardiac insufficiency, associated with impaired contractility, cardiac chamber dilatation and fibrosis. In comparison to age matched non-hypertensive rats LV systolic and diastolic chamber dimensions and filing pressures were increased. In a group of 63 SHR, 54 (85%) died or developed HF by 24 months of age. 37 (59%) had pathologic evidence of HF (cardiac hypertrophy, extensive interstitial fibrosis, and apoptotic myocyte loss) at a mean age of 19±2 months (60, 62).

The genetic factors that cause hypertension remain unidentified (62). The transition from compensated hypertrophy to heart failure is accompanied by changes in cardiac function which are associated with altered active and passive mechanical properties of myocardial tissue: these events define the physiologic basis of cardiac decompensation (60). It has been suggested that excessive fibrosis and increased myocardial stiffness, the overexpression of certain growth factors like transforming growth factor β1, myocyte hypertrophy, increased apoptosis, impaired calcium cycling in association with increased heart rates, elevated energy demand and failure of capillary angiogenesis as consequences of ventricular pressure overload, neurohormonal and renin-angiotensin-aldosterone activation can contribute in the transition from compensated hypertrophy to HF (15, 14, 60, 62). Recently, it has been shown that Angiotensin II may signal across the blood brain barrier to affect neuronal circuits within the nucleus tractus solitarii of the brainstem, a pivotal region regulating both the baroreceptor reflex and set point control of arterial pressure (the depressant action of Angiotensin II is mediated via activation of endothelial nitric oxide synthase releasing NO that promotes release of the inhibitory transmitter-γ-aminobutyric acid) (63).

In these studies, as PARP inhibitor L-2286 was used. L-2286 is derived from 2-mercapto-4(*3H*)-quinazolinone by alkylation with 1-(2-chloroethyl)piperidine (16) (Fig. 1.). L-2286 was choosen, because in in vitro PARP assay it exhibited significantly better PARP inhibitory activity than basic quinazolines such as 4-hydroxyquinazoline or 2-merkapto-4(*3H*)-quinazolinone (17), (Fig. 1).

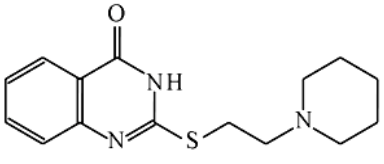

Figure 1. Chemical structure of L-2286 (2-[(2-Piperidine-1-ylethyl)thio]quinazoline-4(3H)-one).

3. Aims of the study

The aim of this work was provide evidence for beneficial in vivo effects of PARP inhibition.

1. To assess cardioprotection afforded by PARP inhibition

a) We tested whether the PARP inhibitor, L-2286 can attenuate the isoproterenol-induced myocardial damage

b) We tested whether the long-term administration of L-2286 can diminish the signs of hypertension induced-HF

c) We compared the protective effect of PARP-inhibition to that of ACE-inhibition against the postinfarction myocardial remodelling.

2. To provide evidence for cardioprotective effects of L-2286, the following parameters were examined:

a) interstitial fibrosis in histological samples

b) phosphorylation state of PI3K/Akt-1^{Ser473}/GSK-3β^{Ser9}, MAPK, PKC cascades by Western blotting

c) echocardiographic parameters with high-resolution imaging system

4. Materials and methods

4.1. Postinfarction heart failure model

Male CFY Sprague-Dawley rats obtained from Charles River Laboratories (Budapest, Hungary) were involved into this study. Myocardial infarction (MI) was induced by subcutaneous injection of 120 mg/kg isoproterenol (ISO, Sigma-Aldrich Co, Budapest, Hungary), while physiological saline (1 ml/kg) was given to control rats intraperitoneally. ISO solutions were prepared with sterile distilled water immediately before injection. After the first ISO injection 6 rat died, further 20 rat died within 24 h after the second ISO injection. 24 hours after the second injection the surviving animals were randomly assigned to receive either 5 mg/kg/day L-2286 (16, 17, 18, 19) (2-[(2-Piperidine-1-ylethyl)thio]quinazoline-4(3H)-one, a gift of Prof. Dr. Kalman Hideg, a water-soluble PARP inhibitor (ISO+L, n=8) or 10 mg/kg/day enalapril maleate (ISO+E, Sigma-Aldrich Co, Budapest, Hungary, n=8), or water (ISO, n=8). The fourth group was an age-matched control group (C, n=8).

4.2. Hypertensive heart failure model

Male 30-week-old SHR rats obtained from Charles River Laboratories (Budapest, Hungary) in the compensated hypertrophic stage were divided randomly into two groups. One group received no treatment (n=47, SHR-C), while the other group recieved L-2286 5 mg/kg/day for 46 weeks (2-[(2-Piperidine-1-ylethyl)thio]quinazoline-4(3H)-one), a water-soluble PARP inhibitor (SHR-L, n=47). The third group was an age-matched normotensive control group (CFY, n=22, Charles River Laboratories, Budapest, Hungary). The dose of L-2286 was based on our previous results with this PARP inhibitor (18, 19). According to these data, L-2286 can exert protective effects against oxidative cell damage in concentration of 10 μM. The serum concentration of L-2286 in the applied dose (5 mg/kg/day) with an estimated average bioavailability is approximately 10 μM in rats. L-2286 was dissolved in drinking water on the basis of preliminary data about the volume of daily consumption, but water was provided ad

libitum throughout the experiment. SHR rats over 40 weeks of age were observed daily, to achieve a description of normal activity, responsiveness to manipulation, weight, respiration and general aspect. Several rats exhibited the following symptoms: lethargy, subcutaneous oedema, and increased respiratory rate. Deaths were recorded daily. Before the administration of L-2286 and at the end of the 46-week treatment period, echocardiographic measurements were performed. Invasive blood pressure measurement was carried out at the beginning (at the age of 30 weeks), at the age of 53-weeks and at the end of the study.

The investigation conforms with to the Guide for the Care and Use of Laboratory Animals published by the U.S. National Institutes of Health (NIH Publication No. 85-23, revised 1996), and was approved by the Animal Research Review Committee of the University of Pecs Medical School.

4.3. Gravimetric parameters

Animals were euthanized with an overdose of ketamine hydrochloride intraperitoneally and heparinized with sodium heparin (100 IU/rat i.p., Biochemie GmbH, Kundl, Austria), sacrified, their blood was collected to determine the concentration of plasma BNP, their hearts were removed, the atria and great vessels were trimmed from the ventricles and weight of the ventricles was measured, which was then normalized to the body mass and to the length of the right tibia (indices of cardiac hypertrophy). The lung wet weight-to-dry weight ratio (an index of pulmonary congestion) were also measured in experimental animals. Hearts were freeze-clamped and were stored at -70°C or fixed in 10% formalin.

4.4. Invasive blood pressure measurements

Five rats from each group in the heart failure model were anaesthetized with ketamine hydrochloride intraperitoneally (Richter Gedeon Ltd., Budapest, Hungary) and a polyethylen catheter (Portex, London, UK) was inserted into their left arteria femoralis. Blood pressure was measured by CardioMed System CM-2005 (Medi-Stim AS, Oslo, Norway).

4.5. Determination of Plasma B-type natriuretic peptide

Blood samples were collected into the Lavender Vacutainer tubes containing EDTA and aprotinin (0.6 TIU/ml of blood) centrifuged at 1600 g for 15 minutes at 4°C to separate plasma. Supernatants were collected and kept at -70°C. Plasma B-type natriuretic peptide-45 levels (BNP-45) were determined by enzyme immunoassay method as the manufacturer proposed (BNP-45, Rat EIA Kit, Phoenix Pharmaceuticals Inc., CA, USA).

4.6. Histology

Formalin-fixed ventricles were sliced and embedded in paraffin. 5 μm thick sections were cut serially from base to apex. Slices at 1 mm intervals were stained. Slices were stained with Picrosirius Red or Masson's trichrome staining to detect the interstitial fibrosis. The sections were mounted on slides and projected at a magnification of 400x and photomicrographs were taken. Collagen Type III was stained as a marker of interstitial fibrosis on frozen sections, 5 μm thick by the Vector M.O.M.™ Kit (Vector Laboratories Inc., Burlingame, CA, USA) staining procedure. After fixing and dehydrating, sections were washed in TRIS-buffered saline (TBS) containing 0,5 % Tween 20, pH 7.6. For blocking the endogenous peroxidase activity, sections were incubated in 3% hydrogen-peroxid then washed in TBS. After 1 h incubation with M.O.M.™ mouse IgG blocking reagent (containing 20 % normal rat serum) sections were washed in TBS, incubated in the working solution of M.O.M.™ diluent for 5 mins. Primary mouse antisera against type collagen III (1:1000, Monoclonal Anti-collagen, Type III, Sigma-Aldrich Co, Budapest, Hungary) diluted in M.O.M.™ diluent reacted at room temperature for 30 mins, folowed by two 2 mins rinses in TBS. Biotinylated Anti-mouse IgG Reagent was then applied for 10 mins sections and were washed twice for 2 mins in TBS. VECTASTATIN ABC Reagent was applied for 5 mins that followed by two 2 mins rinses in TBS. Sections were then stained with Vector NovaRED Substrate (Vector Laboratories Inc., Burlingame, CA, USA) for 5 mins, washed in distilled water, dehydrated, mounted on slides and projected at a magnification of 100x. Sections were quantified with the NIH ImageJ analyzer system.

4.7. Western blot analysis

Fifty miligrams of heart samples were homogenized in ice-cold 50mM Tris buffer, pH 8.0 (containing protease inhibitor cocktail 1:1000, and 50 mM sodium metavanadate, Sigma-Aldrich Co., Budapest, Hungary) and harvested in 2x concentrated SDS-polyacrylamide gel electrophoresis sample buffer. Sodium metavanadate was used as phosphatase inhibitor. Proteins were separated on 10% or 12% SDS-polyacrylamide gel electrophoresis sample buffer. After blocking (2 h with 3% nonfat milk in Tris-buffered saline), membranes were probed overnight at 4°C with antibodies recognizing the following antigenes: phospho-specific Akt-1/protein kinase B-α Ser^{473} (1:1000), Actin (1:10000), phospho-specific glycogen synthase kinase (GSK)-3β Ser^{9} (1:1000), phospho-specific extracellular signal-regulated kinase (ERK 1/2) Thr^{183}-Tyr^{185} (1:1000), phospho-specific p38 mitogen-activated protein kinase (p38-MAPK) Thr^{180}-Gly-Tyr^{182} (1:1000), nonphosphorylated p38 mitogen-activated protein kinase (p38 MAPK) (1:1000), phospho-specific c-Jun N-terminal kinase (JNK) (1:1000), phospho-specific protein kinase C (PKC) (pan) βII Ser^{660} (1:1000), phospho-specific protein kinase C α/βII (PKC α/βII) $Thr^{638/641}$ (1:1000), phospho-specific C δ (PKC δ) Thr^{505} (1:1000), phospho-specific protein kinase C ζ/λ (PKC ζ/λ) $Thr^{410/403}$ (1:1000), phospho-specific protein kinase C ε (PKC ε) Ser^{729} (1:10000), anti poly(ADP-ribose) (anti-PAR, 1:5000). Antibodies were purchased from Cell Signaling Technology, Beverly, MA, USA except from anti-actin which was bought from Sigma-Aldrich Co, Budapest, Hungary, phospho-specific anti-protein kinase C ε, which was purchased from Upstate, London, UK and anti-PAR, which was purchased from Alexis Biotechnology, London, UK. Membranes were washed six times for 5 min in Tris-buffered saline (pH 7,5) containing 0.2% Tween (TBST) before addition of goat anti-rabbit horseradish peroxidase-conjugated secondary antibody (1:3000 dilution, Bio-Rad, Budapest, Hungary). The antibody-antigen complexes were visualized by means of enhanced chemiluminescence. After scanning, results were quantified by NIH ImageJ program.

4.8. Noninvasive evaluation of cardiac function

At the beginning of the experimets all animals were examined by echocardiography to exclude rats with any heart abnormalities. Transthoracic two-dimensional echocardiography was performed under inhalation anesthesia at the beginning of the experiment and on the day of sacrifice. Rats or mice were lightly anesthetized with a mixture of 1.5% isoflurane and 98.5% oxygen. The chest of animals was shaved, acousting coupling gel was applied and warming pad was used to maintain normothermia. Animals were imaged in the left lateral decubitus position. Cardiac dimensions and functions were measured from short- and long-axis views at the mid-papillary level by a VEVO 770 high resolution ultrasound imaging system (VisualSonics, Toronto, Canada) - equipped with a 25 MHz transducer. LV fractional shortening (FS), ejection fraction (EF), LVEDV, LVESV, and the thickness of septum and posterior wall were determined. FS (%) was calculated by $100x((LVID_d-LVID_s)/LVID_d)$ (LVID means LV inside dimension), EF (%) was calculated by $100x((LVvol_d-LVvol_s)/LVvol_d)$.

4.9. Statistical analysis

All data are expressed as mean±SEM. Comparisons among groups were made using Student's t test or one-way ANOVA (SPSS for Windows 11.0). To post hoc comparison Bonferroni test was choosen. Survival was depicted graphically using Kaplan-Meier survival curves and compared using log-rank test. Values of $p<0.05$ were considered statistically significant.

5. Results

5.1. L-2286 favourably influences the gravimetric parameters

In our first study (postinfarction heart failure model), gravimetry performed 12 weeks after ISO-induced myocardial infarction showed significantly elevated ventricular weight ($p<0.05$), as well as ventricular weight normalized to body weight ($p<0.01$) and to tibia length ($p<0.05$) compared to control group. Both L-2286 (L, PARP inhibitor) and enalapril-maleate (E, angiotensin-converting enzyme inhibitor) treatment significantly mitigated these unfavorable changes (Table 1).

	Control	ISO	ISO+L	ISO+E
BW (g)	378.75±11.09	441±9.81[a]	399±9.762[b]	397.5±11.87[b]
WV (g)	0.90±0.012	1.15 ±0.019[a]	0.95±0.029[b]	0.96±0.019[b]
WV/BW (mg/g)	2.31 ±0.16	2.79 ±0.27[c]	2.35±0.21[d]	2.37±0.23[d]
WV/TL (mg/mm)	20.68 ±1.12	26.64 ±1.35[c]	21.52±1.19[b]	21.60±1.14[b]
Plasma BNP (ng/ml)	2.23±0.88	2.85±0.041[c]	2.56±0.042[b]	2.56±0.055[b]

Table 1

Effect of L-2286 (L, PARP inhibitor) and enalapril-maleate (E, angiotensin-converting enzyme inhibitor) on gravimetric parameters and the levels of plasma BNP 12 weeks after ISO (isoproterenol) induced myocardial infarction (n=8). BW: body weight, WV: weight of ventricles, TL: length of right tibia, WV/BW: weight of ventricles/body weight ratio, WV/TL: weight of ventricles/ length of right tibia. Values are means ± S.E.M. ISO: rats 12 weeks after ISO administration; ISO+L: rats treated with L-2286, 12 weeks after ISO administration; ISO+E: rats treated with enalapril-maleate, 12 weeks after ISO administration. [a] $p<0.05$ (vs. Control group), [b]$p<0.05$ (vs. ISO), [c]$p<0.01$ (vs. Control group), [d]$p<0.01$ (vs. ISO group).

In our second investigation (hypertensive heart failure model), the body weight of CFY rats was significantly higher than the body weight of SHR rats at the beginning of the study (CFY: 387.5±4.78 g, SHR-C: 345.25±8.71 g, SHR-L: 334.44±8.67 g, $p<0.05$, 30-week-old rats). Similar results were obtained at the end of the study (CFY: 408.75±6.14 g, SHR-C: 356.8±5.61 g, SHR-L: 367.67±9.7 g, $p<0.05$ CFY vs. SHR groups, 76-week-old rats). Treatment with PARP inhibitor somewhat increased the body weight (SHR-L group vs. SHR-C group) but the changes were not significant. At the end of the study (76 week-old rats), heart weights (HW), weights of ventricles (WV) were significantly increased in the SHR group compared to the CFY group (HW (g): CFY: 1.22±0.04, SHR-C:1.61±0.05, SHR-L: 1.41±0.03, $p<0.01$ CFY vs. SHR-C, $p<0.05$ SHR-L vs. CFY, SHR-C, WV (g): CFY: 1.11±0.03, SHR-C: 1.43±0.04, SHR-C: 1.29±0.03, $p<0.01$ CFY vs. SHR-C, $p<0.05$ SHR-L vs. CFY, SHR-C), these parameters were significantly decreased by L-2286 treatment. The ratios of weight of ventricles to body weight (WV/BW) and weight of ventricles to length of right tibia (WV/TL) were also significantly increased (WV/BW (g/g): CFY: 2.71±0.09, SHR-C: 3.99±0.06, WT/TL (mg/mm): CFY: 23.53±0.77, SHR-C: 31.16±0.68 $p<0.01$ CFY vs. SHR-C) compared to the CFY group, and were diminished significantly by this PARP inhibitor (WV/BW (g/g): SHR-L: 3.52±0.09, WV/TL (mg/mm): SHR-L: 28.26±0.65 $p<0.01$ vs. CFY and $p<0.05$ vs. SHR-C). The ratio of lung wet weight-to-dry weight was enhanced in the SHR groups significantly (CFY: 4.65±0.1 g/g, SHR-C: 5.25±0.07 g/g, $p<0.05$ CFY vs. SHR-C), and was favorably influenced by L-2286 (SHR-L: 5.03±0.04 g/g, $p<0.01$ vs. CFY and $p<0.05$ vs. SHR-C) (Table 2). These parameters of the SHR groups indicated not only the presence of cardiac hypertrophy, but also the presence of pulmonary congestion (54). During the sacrifice HF diagnosis was confirmed by the presence of ascites, internal congestion, hepatomegaly and pleural effusion (54), which occurred very frequently in the SHR-C group.

The survival rate was also significantly ($p<0.01$) improved by the administration of L-2286. Only the curves of the two SHR groups were compared, because there was no mortality in the CFY group (Fig. 2).

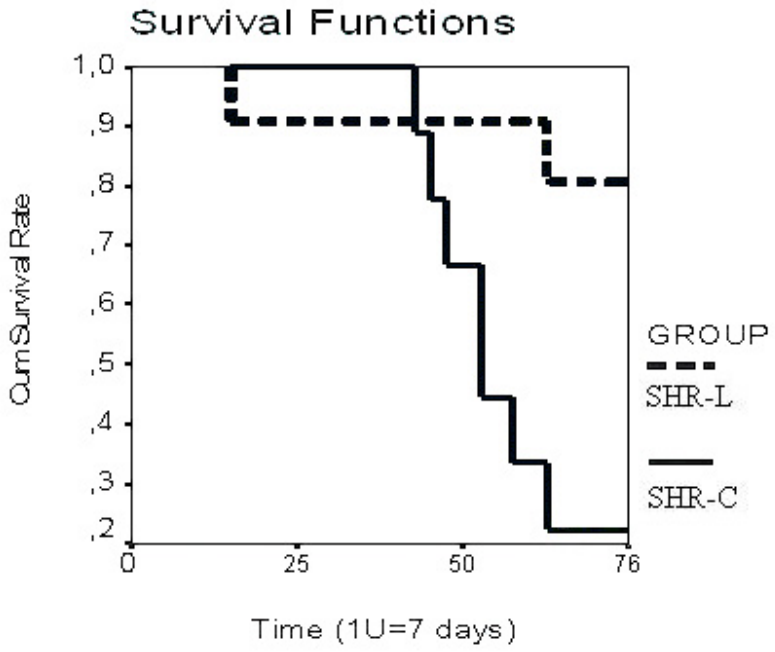

Figure 2. Kaplan-Meier survival curves of SHR-C and SHR-L groups. Group SHR-C means 76 week-old spontaneously hypertensive rats. Group SHR-L means 76 week-old spontaneously hypertensive rats treated with L-2286 for 46 week. The experiment was started with 30 week-old SHRs. 1 time unit means 7 days.

	CFY	SHR-C	SHR-L
BW^{30w} (g)	387.5±4.78	345.25±8.71[b]	334.44±8.67[b]
BW^{76w} (g)	408.75±6.14	356.8±5.61[b]	367.67±9.7[b]
HW^{76w} (g)	1.22±0.04	1.61±0.05[a]	1.41±0.03[b,c]
WV^{76w} (g)	1.11±0.03	1.43±0.04[a]	1.29±0.03[b,c]
WV/BW^{76w} (g/g)	2.71±0.09	3.99±0.06[a]	3.52±0.09[a,c]
WV/TL^{76w} (mg/mm)	23.53±0.77	31.16±0.68[a]	28.26±0.65[a,c]
Lung wet weight/dry $weight^{76w}$ (g/g)	4.65±0.1	5.25±0.07[a]	5.03±0.04[a,c]
p-BNP^{76w} (ng/ml)	2.03±0.06	2.71±0.07[a]	2.21±0.06[a,d]

Table 2.
Effect of L-2286 treatment on gravimetric parameters and on plasma-BNP in CFY and SHR. CFY: normotensive age-matched control rats, n=7, SHR-C: spontaneously hypertensive rats (SHR) 76 week-old SHR control rats, n=7, SHR-L: 76 week-old SHR treated with L-2286, for 46 weeks, n=26. $BW^{30w, 76w}$: body weight of 30 week-old and 76 week-old rats, HW^{76w}: Heart weight of 76 week-old rats, WV^{76w}: weights of ventricles of 76 week-old rats, TL^{76w}: lenght of right tibia of 76 week-old rats, p-BNP^{76w}: plasma brain natriuretic peptid of 76 week-old rats. Values are means±S.E.M. [a]<0.01 (vs. CFY group), [b]<0.05 (vs. CFY group), [c]<0.05 (vs. SHR-C), [d]<0.01 (vs. SHR-C)

5.2. Effect of L-2286 on the level of p-BNP

In postinfarction heart failuer model, 12 weeks after MI p-BNP significantly elevated in ISO group compared to control group ($p<0.01$). ACE and PARP inhibition decreased significantly this elevation ($p<0.05$) suggesting that both treatments are able to diminish the severity of postinfarction heart failure (Table 1.).

In hypertensive HF model, the level of plasma-BNP was significantly elevated in the SHR groups ($p<0.01$ CFY vs. SHR groups) compared to CFY group and this elevation was significantly decreased by L-2286 treatment ($p<0.01$ SHR-C vs. SHR-L (Table 2.).

5.3. Effect of L-2286 on interstitial collagen deposition

In myocardial infarction model, histologic analysis revealed marked interstitial fibrosis in ISO group compared to control group (28.8%±2.78 vs 12.96%±1.5 $p<0.01$). All treatment attenuated significantly this phenomenon (ISO+L: 21%±2.74 $p<0.05$, ISO+E: 23,56%±2.38 $p<0.05$). Administrating L-2286 after MI was slightly better to prevent the development of interstitial fibrosis than enalapril, but the difference between the two types of treatment was not statistically significant (Fig. 3).

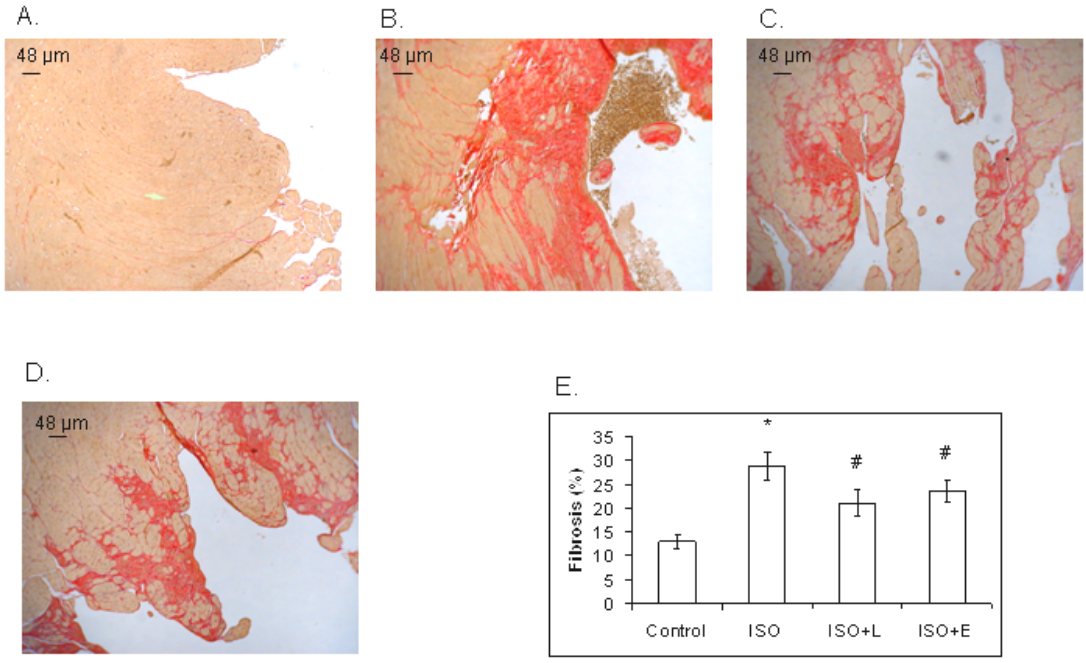

Figure 3. Effect of L-2286 and E (enalapril-maleate) on ISO-induced (isoproterenol) interstitial fibrosis. Sections obtained from hearts of Control (A, n=4), ISO (B, n=4): 12 weeks after ISO injections, ISO+L-2286 (C, n=4): L-2286-treated rats, 12 weeks after ISO injections, ISO+E (D, n=4): E treated rats, 12 weeks after ISO injections. Sections were stained with Picro Sirius Red, and denzitometric evaluation of Picro Sirius Red stained sections (E) are shown. Magnifications 20xfold. Scale bars mean 48 µm. Areas with collagen are red, while areas without collagen deposition are brown. Values are means ± S.E.M., *, significant difference from control samples ($p<0.01$). #, significant difference from ISO-treated samples ($p<0.05$).

In hypertensive heart failure model, the highest value of interstitial collagen deposition was obtained from SHR-C rats ($p<0.01$ vs CFY), the deposition of collagen was significantly ($p<0.05$) moderated by L-2286 (Fig. 4).

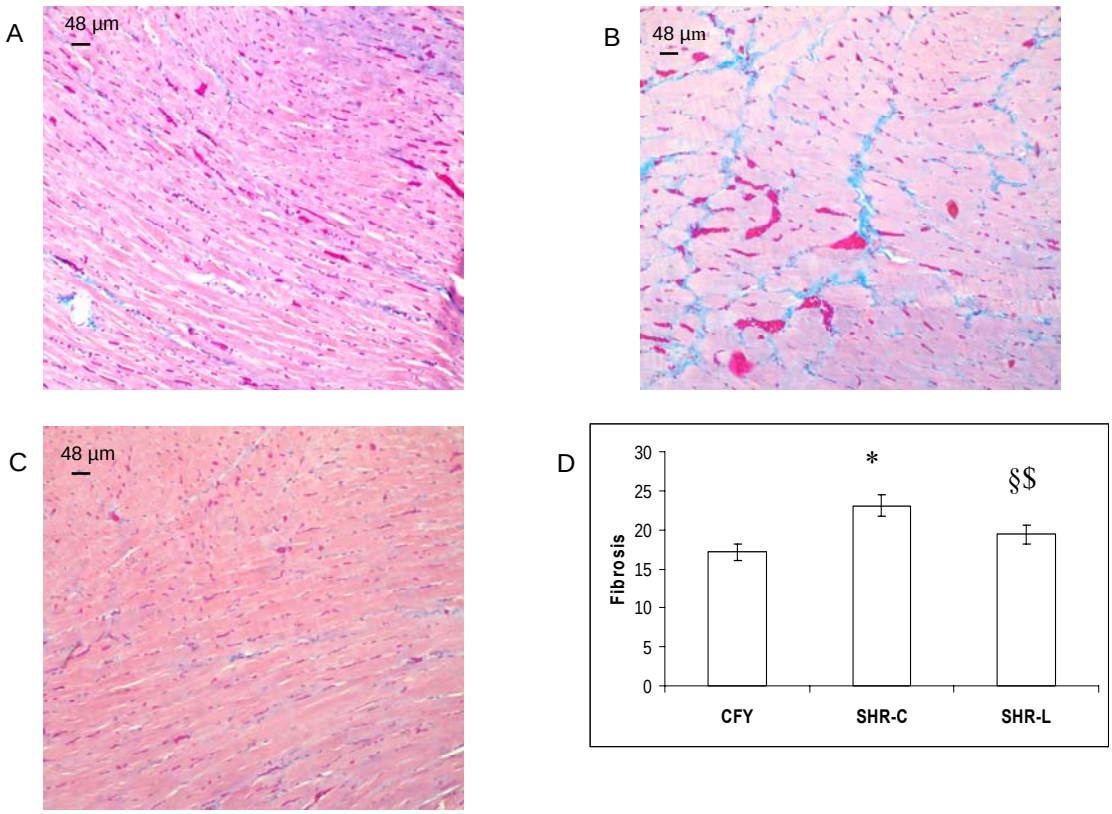

Figure 4. Effect of L-2286 treatment on the deposition of interstitial collagen (%). Representative histologic sections stained with Masson's trichrome (n=4). Magnification 20xfold. Scale bars means 48 µm. CFY (A): normotensive age-matched control rats. SHR-C (B): 76 week-old spontaneously hypertensive rats, SHR-L (C): 76 week-old spontaneously hypertensive rats treated with L-2286 for 46 week. D: Denzitometric evaluation of sections is shown. $^{*}p<0.01$ vs CFY, $^{\S}p<0.05$ vs CFY, $^{\$}p<0.05$ vs SHR-C.

5. 4. Effect of L-2286 administration on Akt-1^{Ser473}/GSK-3β^{Ser9} phophorylation and ADP-ribosylation

In postinfarction HF model, Akt-1^{Ser473} was slighty phosphorylated in the control group and became moderately phosphorylated in the ISO group ($p<0.01$). Phosphorylation of Akt-1^{Ser473} elevated markedly in ISO+L group ($p<0.01$ vs. ISO group) and it was also strongly increased in ISO+E group ($p<0.01$ vs. ISO group). PARP inhibition with L-2286 caused significantly greater phosphorylation and activation of Akt-1^{Ser473} compared to ACE-inhibition with enalapril ($p<0.05$ vs ISO+E). Akt-1^{Ser473} is one of the upstream kinases of GSK-3β^{Ser9}, which can inhibit the activity of the latter through phophorylation (Fig. 5).

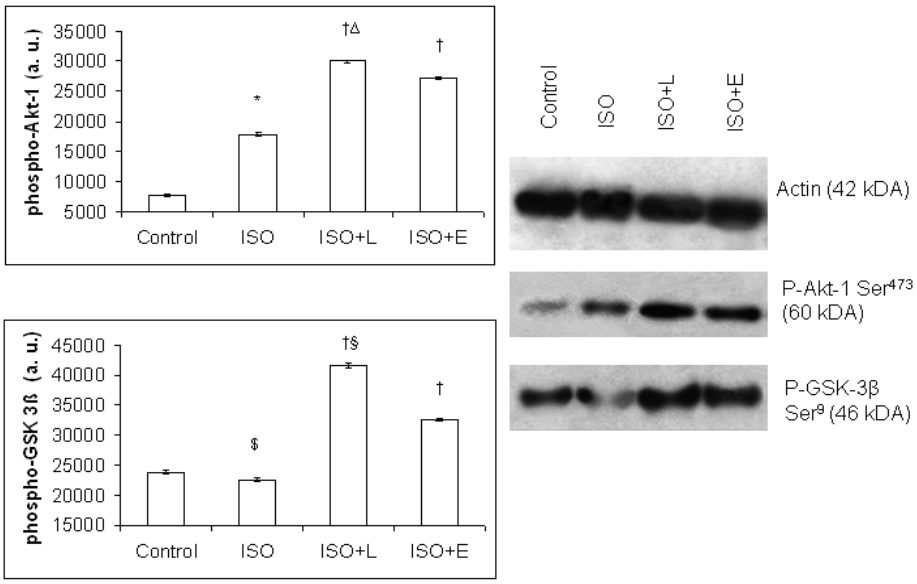

Figure 5. Effect of L-2286, E (enalapril-maleate) on Akt-1-GSK-3β pathway. Representative Western blot analysis of Akt-1 (A, B) and GSK-3β (A, C) phosphorylation and densitometric evaluations are shown (n=4). Actin is shown as loading control (A). Values are means ± S.E.M., *, significant difference from control sample ($p<0.01$). $, significant difference from control samples ($p<0.05$). †, significant difference from ISO-treated (isoproterenol) samples $p<0.01$). Δ, significant difference from ISO+E sample ($p<0.05$). §, significant difference from ISO+E samples ($p<0.01$). (a. u. means arbitrary units). ISO: 12 weeks after ISO injections, ISO+L: L-2286-treated rats, 12 weeks after ISO injections, ISO+E: E treated rats, 12 weeks after ISO injections.

The phosphorylation of GSK-3β^{Ser9} was mitigated slightly in ISO group compared to control (NS vs ISO group). Both L-2286 and enalapril elevated significantly the

phosphorylation of GSK-3β^{Ser9} ($p<0.01$ vs C and ISO group), however the strongest inhibition of GSK-3β^{Ser9} was achieved by the administration of L-2286 ($p<0.01$ vs. ISO+E group) (Fig 5).

In hypertensive heart failure model, Akt-1^{Ser473} was activated in elderly CFY rats ($p<0.01$ vs. SHR groups), while its activity was downregulated in SHR-C rats, but the phosphorylation of it was increased in ($p<0.01$) SHR-L animals. Similar results were obtained from analysis of GSK-3β^{Ser9} phosphorylation, which is one of the downstream target of Akt-1^{Ser473} (Fig 6).

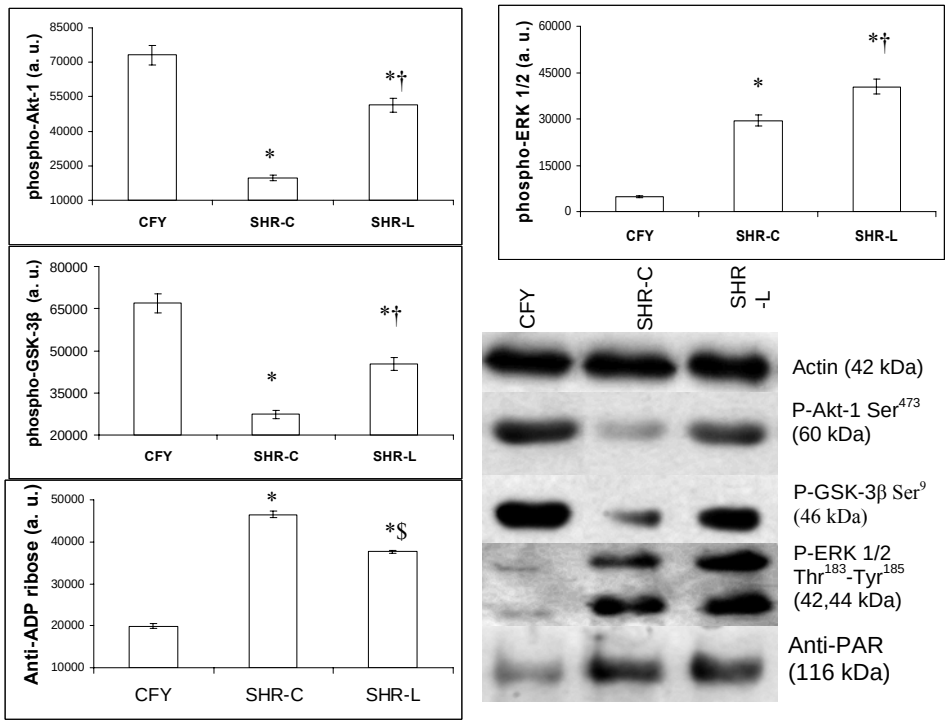

Figure 6. Effect of L-2286 treatment on Akt-1^{Ser473}-GSK-3β^{Ser9} pathway and ERK 1/2$^{Thr183\text{-}Tyr185}$. Representative Western blot analysis of Akt-1^{Ser473}, GSK-3β^{Ser9} and ERK 1/2 $^{Thr183\text{-}Tyr185}$ phosphorylation, anti-PAR and densitometric evaluation is shown (n=4). Actin showing as loading control. Values are means±S.E.M. CFY: normotensive age-matched control rats. SHR-C: 76 week-old spontaneously hypertensive rats, SHR-L: 76 week-old spontaneously hypertensive rats treated with L-2286 for 46 week. $^{*}p<0.01$ vs CFY, $^{\dagger}p<0.01$ vs SHR-C, $^{\S}p<0.05$ vs CFY, $^{\$}p<0.05$ vs SHR-C.

In the last experiment, to analyze the effectivity of L-2286, the ADP-ribosylation of the samples were detected. The smallest degree of this type of ribosylation was present in SHR-L group, and this attenuation was significantly different compared to SHR-C group ($p<0.05$) (SHR 76 week-old rats: Fig. 6).

Western blot analysis of ADP-ribosylated heart proteins revealed that the ADP-ribosylation of SHR-C heart samples were the highest. This elevation was significantly decreased ($p<0.05$ SHR-C vs SHR-L group) by L-2286 treatment.

5.5. Effect of L-2286 on the MAPK pathways

In our first experiment (post MI remodelling model), ERK $1/2^{Thr183\text{-}Tyr185}$ was modaretely phosphorylated in control animals and became less phosphorylated 12 weeks after MI in the ISO group ($p<0.05$ C vs ISO group). Both L-2286 and enalapril treatment resulted in a further augmented phosphorylation of ERK$1/2^{Thr183\text{-}Tyr185}$ ($p<0.01$ vs ISO), however the strongest phosphorylation could be observed in the ISO+L group ($p<0.01$ vs ISO+E) (Fig.7).

Phosphorylation of p38-$MAPK^{Thr180\text{-}Gly\text{-}Tyr182}$ was slightly decreased in ISO group (NS vs. C) and it was increased by both treatments ($p<0.01$ vs ISO). The difference of the phosphorylation of p38-$MAPK^{Thr180\text{-}Gly\text{-}Tyr182}$ was not statistically significant between ISO+L and ISO+E groups (Fig. 7). In case of c-jun N-terminal kinase (JNK), the phosphorylation was decreased in ISO group ($p<0.05$ vs C). This attenuation was augmented by both L-2286 and enalapril treatment ($p<0.05$ vs ISO) (data not shown).

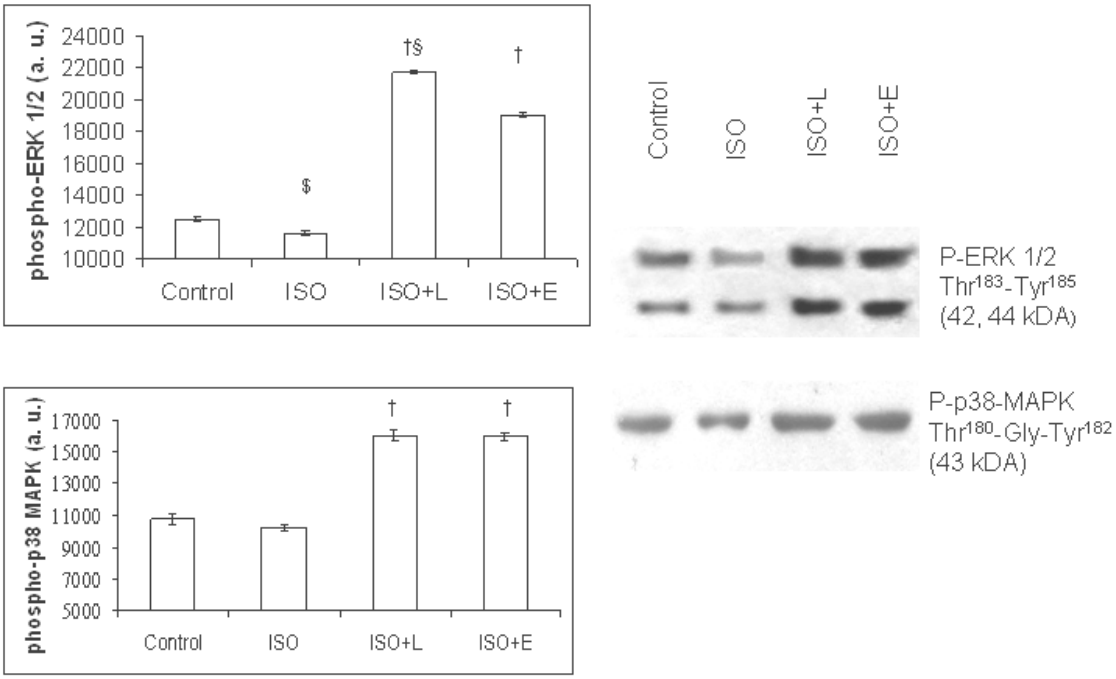

Figure 7. Effect of L-2286, E (enalapril-maleate) on ERK 1/2 and p38-MAPK pathways. Representative western blot analysis of ERK 1/2 (A, B) and p38-MAPK (A, D) and densitometric evaluation are shown (n=4). Values are means ± S.E.M., *, significant difference from control sample ($p<0.01$). $, significant difference from control samples ($p<0.05$). †, significant difference from ISO-treated (isoproterenol) samples $p<0.01$). §, significant difference from ISO+E samples ($p<0.01$). (a. u. means arbitrary units). ISO: 12 weeks after ISO injections, ISO+L: L-2286-treated rats, 12 weeks after ISO injections, ISO+E: E treated rats, 12 weeks after ISO injections.

In hypertensive heart failure model, the modest phosphorylation of the examined –p38-MAPK$^{Thr183\text{-}Gly\text{-}Tyr185}$, JNK, ERK 1/2$^{Thr183\text{-}Tyr185}$ –MAPKs pathways occured in CFY rodents ($p<0.01$ vs SHR groups). The phosphorylation of p38-MAPK$^{Thr183\text{-}Gly\text{-}Tyr185}$ (Fig. 8) and JNK (data not shown) of SHR-C rats was the highest, and these alterations were attenuated by L-2286 treatment significantly ($p<0.01$).

The phosphorylation of ERK 1/2$^{Thr183\text{-}Tyr185}$ was raised ($p<0.01$) in SHR-C group compared to CFY group and this was further enhanced ($p<0.01$) by L-2286 administration compared to SHR-C (Fig. 6).

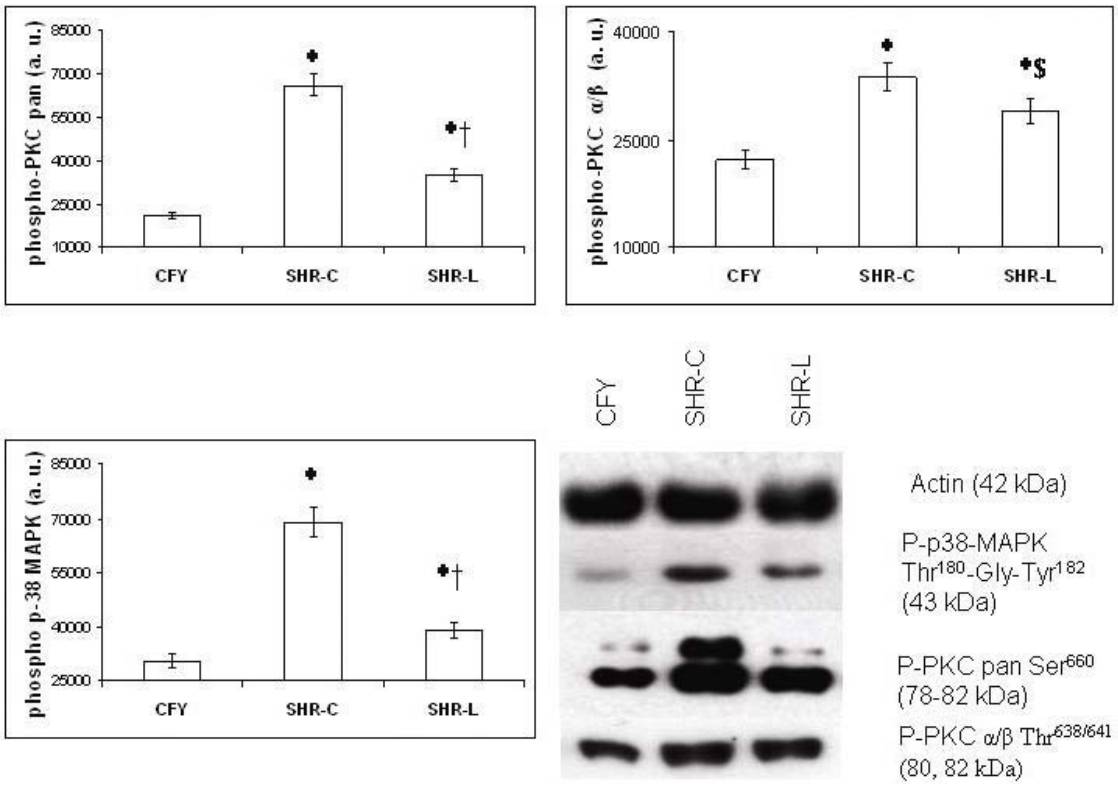

Figure 8. Effect of L-2286 on the phosphorylation of p38-MAPK$^{Thr180\text{-}Gly\text{-}Tyr182}$ and PKC pathways. Representative Western blot analysis of p-38-MAPK $^{Thr180\text{-}Gly\text{-}Tyr182}$, PKC pan βII^{Ser660} and PKC α/βII$^{Thr638/341}$ phosphorylation and densitometric evaluation is shown (n=4). Actin showing as loading control. Values are means±S.E.M. CFY: normotensive age-matched control rats. SHR-C: 76 week-old spontaneously hypertensive rats, SHR-L: 76 week-old spontaneously hypertensive rats treated with L-2286 for 46 week. $^{*}p<0.01$ vs CFY, $^{\dagger}p<0.01$ vs SHR-C, $^{\S}p<0.05$ vs CFY, $^{\$}p<0.05$ vs SHR-C.

5.6. Effect of L-2286 treatment on PKC pathways

In our postinfarction heart failure model, the phosphorylation of PKC pan βII^{Ser660} was strongly elevated in ISO group ($p<0.01$) compared to control animals. Both of the two treatments (L-2286 and ENA) reduced significantly this augmentation ($p<0.01$ vs. ISO). The lowest phosphorylation could be observed in ISO+L group ($p<0.01$ vs ISO+E) (Fig. 10).

The similar result was revealed in the case of PKC $\alpha/\beta II^{Thr638/641}$, PKC δ^{Thr505} and PKC ζ/λThr410/403. In case of PKC ζ and PKC ι/λ, we used a combined antibody (i.e. PKC ζ/λ $Thr^{410/403}$), which did not discriminate between PKC ζ and PKC ι/λ which were structurally highly homologous to PKC ζ in the COOH-terminal end of the molecule (35) (Fig. 9). In control animals PKC ε^{Ser729} was phosphorylated but in ISO group PKC ε showed a significantly lower phosphorylation state ($p<0.01$ vs. C). Both L-2286 and enalapril increased the phosphorylation of PKC ε^{Ser729} significantly ($p<0.01$ vs ISO). However PARP-inhibition exerted a markedly stronger activation of PKC ε^{Ser729} compared to ACE-inhibition with enalapril ($p<0.01$ vs ISO+E).

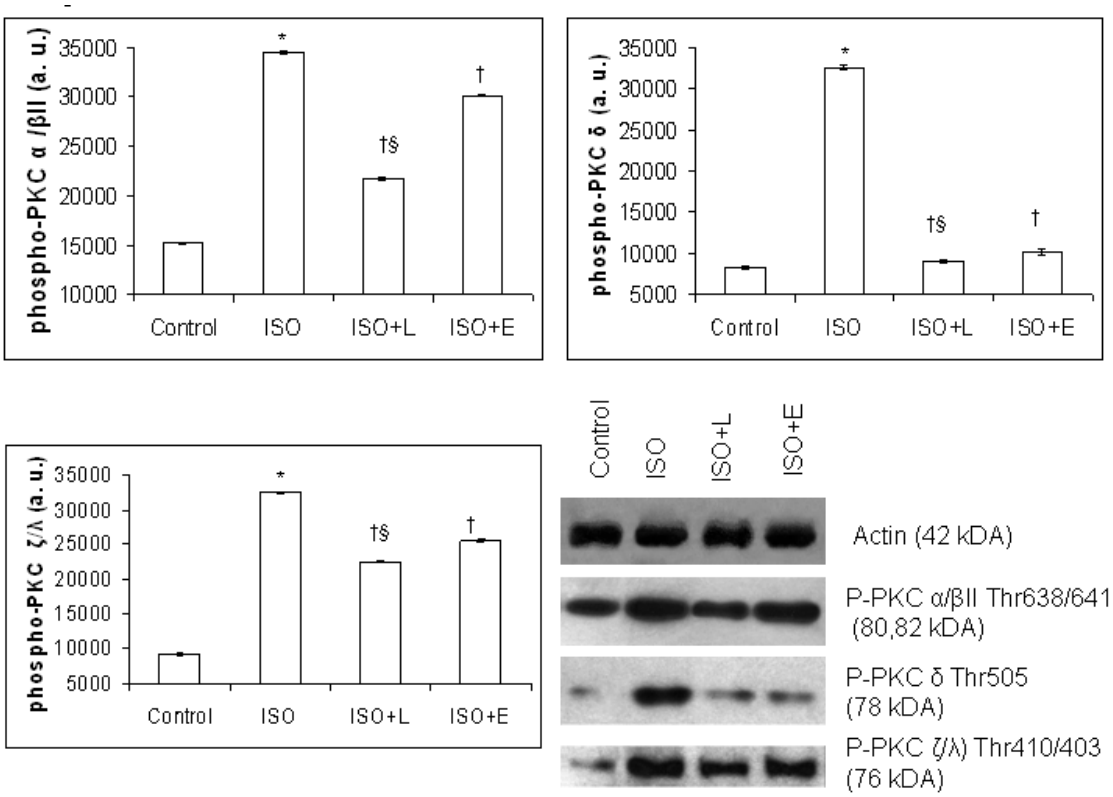

Figure 9. Effect of ISO (isoproterenol) on the phosphorylation of PKC α/β, PKC δ and PKC ζ/λ, while both L-2286 and E (enalapril-maleate) administration decreased it and the effect of E and L-2286 on PKC ε and PKC pan βII after 12 weeks of ISO injections. Representative Western blot analysis of PKC α/β, PKC δ, PKC ζ/λ, ε, pan βII and densitometric evaluation are shown (n=4). Actin is shown as a loading control (A). Values are means ± S.E.M., *, significant difference from control sample ($p<0.01$). $, significant difference from control samples ($p<0.05$). †, significant difference from ISO-treated samples $p<0.01$). §, significant difference from ISO+E samples ($p<0.01$). (a. u. means arbitrary units). ISO: 12 weeks after ISO injections, ISO+L: L-2286-treated rats, 12 weeks after ISO injections, ISO+E: E treated rats, 12 weeks after ISO injections.

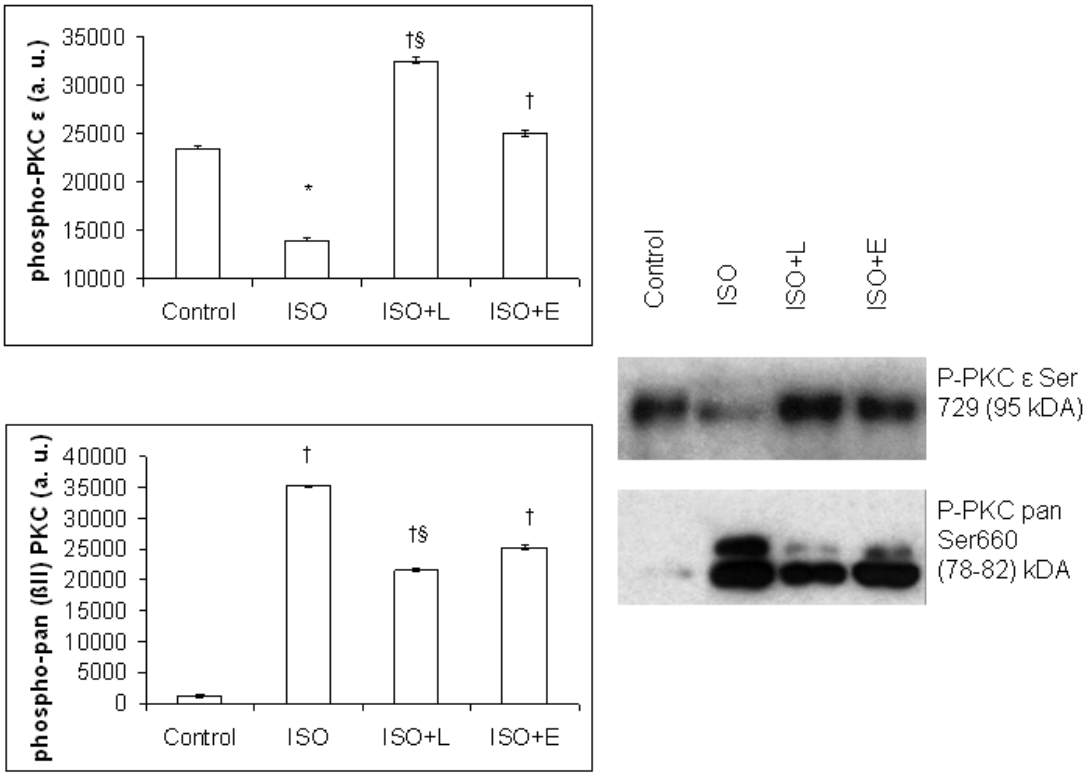

Figure 10. Effect of L-2286 and E treatment on PKC ε and PKC pan pathway. Representative Western blot analysis of PKC ε, PKC pan and densitometric evaluation are shown. PKC ε is shown as a loading control. Values are means ± S.E.M., *, significant difference from control sample ($p<0.01$). $, significant difference from control samples ($p<0.05$). †, significant difference from ISO-treated samples $p<0.01$). §, significant difference from ENA-treated samples ($p<0.01$). (a. u. means arbitrary units).

In our second investigation (hypertensive heart failure model), the phosphorylation of PKC pan βII^{Ser660}, PKC $\alpha/\beta II^{Thr638/641}$, δ^{Thr505}, ε^{Ser729}, ζ was the lowest in CFY rodents ($p<0.01$ vs SHR groups). The activity of PKC pan βII^{Ser660}, $\alpha/\beta II^{Thr638/641}$, δ^{Thr505}, and ζ was augmented in SHR-C rodents, but these elevations were significantly moderated by L-2286 treatment ($p<0.01$ PKC pan βII^{Ser660} and ζ, $p<0.05$ PKC $\alpha/\beta II^{Thr638/641}$,$\delta^{Thr505}$) (Fig. 11). On the other hand, the enhanced phosphorylation of PKC ε^{Ser729} was further increased significantly ($p<0.01$) by L-2286 administration (Fig. 11).

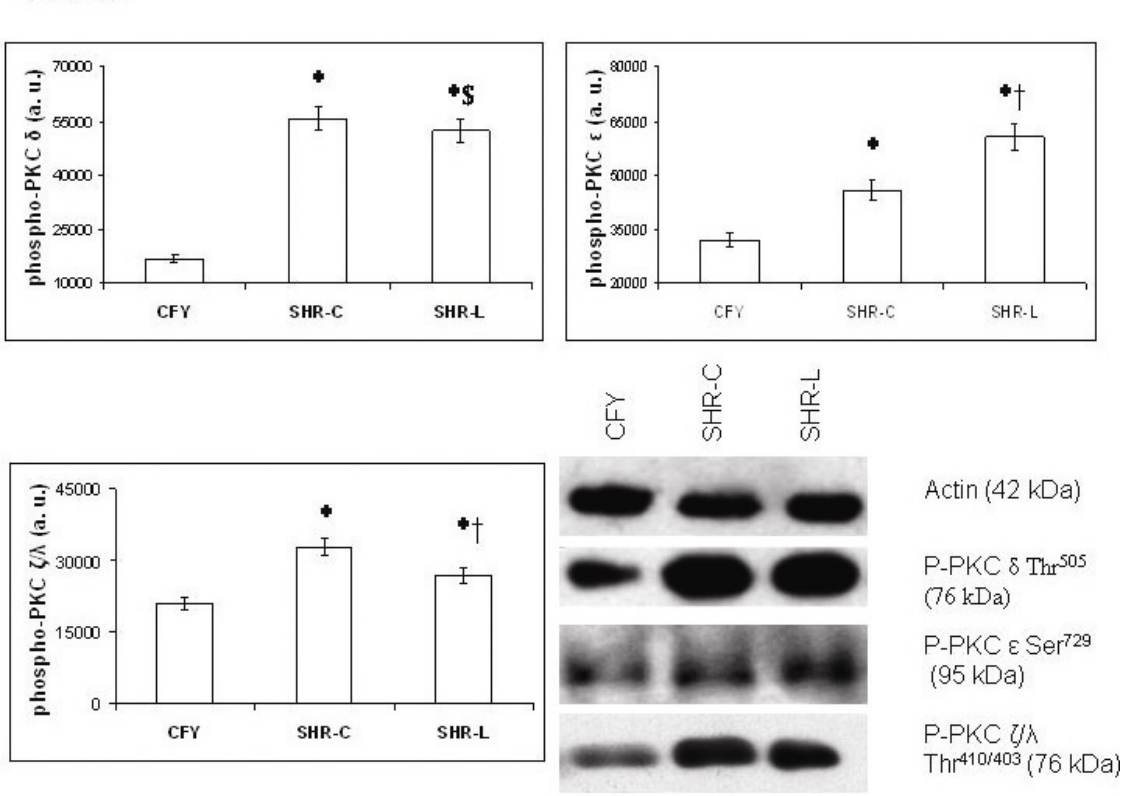

Figure 11. Effect of L-2286 administration of PKC isoenzymes. Representative Western blot analysis of PKC δ^{Thr505} and PKC ε^{Ser729}, $\zeta/\lambda^{410/403}$ phosphorylation and densitometric evaluation is shown (n=4). Values are means±S.E.M. CFY: normotensive age-matched control rats. SHR-C: 76 week-old spontaneously hypertensive rats, SHR-L: 76 week-old spontaneously hypertensive rats treated with L-2286 for 46 week. $^{*}p<0.01$ vs CFY, $^{\dagger}p<0.01$ vs SHR-C, $^{\S}p<0.05$ vs CFY, $^{\$}p<0.05$ vs SHR-C.

5.7. Effect of L-2286 administration on cardiac function

In postinfarction HF model, before the administration of enalapril and L-2286 (and after the second ISO injection), there were no significant differences among the two groups (data not shown). After 12 weeks, both EF and FS were markedly mitigated in postinfarction animals (ISO group) compared to healthy animals (Control group, $p<0.01$). These unfavourable changes were improved by L-2286 treatment (EF, FS; $p<0.01$ vs ISO). Enalapril could exert a significantly lower protection against the worsening of systolic LV function ($p<0.05$ vs. ISO+L).

In all postinfarction groups (ISO, ISO+L, ISO+E) LVEDV was increased significantly ($p<0.01$ vs. C). Neither L-2286, nor enalapril could reduce this unfavorable effect. LVESV was also increased in ISO group. Administration of L-2286 caused a highly significant reduction in LVESV ($p<0.01$ vs ISO), enalapril however exerted a less marked effect on it ($p<0.01$ vs ISO+L group).

Ventricular hypertrophy developed in postinfarction animals (ISO group) which was characterized by the thickness of septum and posterior wall (PW, $p<0.05$ vs. C). Both ACE- and PARP-inhibitors could attenuate the development of left ventricular hypertrophy ($p<0.05$ vs ISO) (Table 3, Fig. 12).

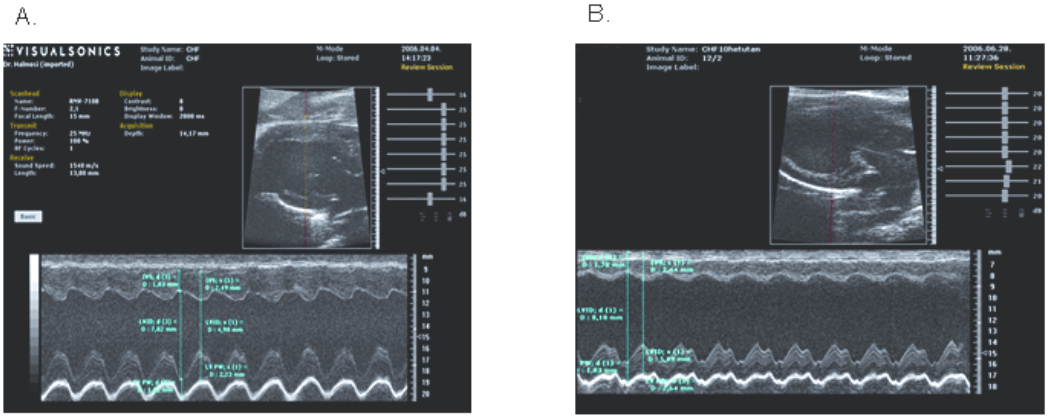

Figure 12. Examples of echocardiographic findings for the control (A, n=8), ISO-treated (isoproterenol, B, n=8) rats. IVS (d), (s): interventricular septum thickness in diastole, systole. LVID (d): left ventricular end-diastolic diameter, LVID (s): left ventricular end-systolic diameter. LV PW (d), (s): thickness of left ventricular posterior wall diastole, systole. ISO: 12 weeks after ISO injections.

In the hypertensive heart failure model, there was no significant difference in LV systolic function (EF, FS) between the CFY and SHR groups at the age of 30-weeks (EF (%): CFY: 68.10±0.90 and SHR^{30w}: 68.33±1.75, FS (%): CFY: 38.45±4.38 and SHR^{30w}: 39.10±3.33). Heart rate did not differ significantly during anesthesia (CFY: 269±18, SHR 272±15 heart rate was decreased because of the isoflurane) between the groups. However, LVESV and LVEDV, the thickness of the PW and septum, RWT and LV mass (indicating ventricular hypertrophy) also increased significantly in SHR ($p<0.05$ CFY vs SHR) (Table 4).

	Control	ISO	I+L	I+E	I+E+L
EF (%)	68.9±1.8	53.01±0.99[c]	70.41±2.56[d]	60.08±1.63[b,e]	61.91±2.75[b,e]
FS	40.05±1.55	28.37±0.62[c]	42.35±1.81[d]	33±1.33[b,e]	35.96±1.93[b,e]
LVEDV	283.13±6.73	363.46±6.54[c]	385.31±7.31[b]	365.6±13.47[b]	414.67±7.31[b]
LVESV	86.23±6.23	164.85±7.85[c]	98.59±4[d]	157.14±4.89[b]	142.06±4.96[b]
Septum (mm)	1.75±0.041	1.95±0.067[a]	1.62±0.062[b]	1.63±0.061[b]	1.68±0.05[b]
PW (mm)	1.76±0.039	1.93±0.068[a]	1.68±0.072[b]	1.59±0.041[b]	1.82±0.057

Table 3. L-2286, ENA (enalapril) and their combination significantly improved echocardiographic parameters after ISO injections. Conditions for performing echocardiographic parameters are detailed in Materials and methods. EF: ejection fraction, FS: fractional shortening, LVEDV: left ventricular (LV) end-diastolic volume, LVESV: LV end-systolic volume, Septum: thickness of septum, PW: thickness of posterior wall. ISO: rats 12 weeks after ISO injections; I+L: rats treated with L-2286, 12 weeks after ISO injections; I+E: rats treated with ENA, 12 weeks after ISO injections; I+E+L: rats treated with L-2286 and ENA, 12 weeks after ISO injections; Values are means ± S.E.M., [a] $p<0.05$ (vs. Control group), [b] $p<0.05$ (vs. ISO), [c] $p<0.01$ (vs. Control group), [d] $p<0.01$ (vs. ISO group), [e] $p<0.05$ (vs I+L group)

	CFY^{30w}	SHR^{30w}
EF (%)	68.1±0.9	68.33±1.75
FS (%)	38.45±4.38	39.1±3.33
LVEDV (ml)	278.55±15.78	339.84±14.65[a]
LVESV (ml)	86.45±9.02	98.23±10.4[a]
PW (mm)	1.6±0.07	2.11±0.09[a]
Septum (mm)	1.48±0.06	1.83±0.08[a]
RWT	0.4±0.05	0.51±0.02[a]
LV mass (uncorr, mg)	999.57±61.3	1250.58±78.78[a]
LV mass/BW (mg/g)	2.59±0.9	3.69±0.06[a]

Table 4. Echocardiographic parameters of 30 week-old male normotensive CFY Sprague-Dawley (CFY, n=7) and 30 week-old spontaneously hypertensive rats (SHR, n=15). EF: ejection fraction, FS: fractional shortening, LVEDV: left ventricular (LV) end-diastolic volume, LVESV: LV end-systolic volume, Septum: thickness of septum at, PW: thickness of posterior wall, RWT: relative wall thickness, LV mass: weights of LV, BW: body weight. Values are mean±S.E.M. [a] $p<0.05$ (vs. CFY group)

At the end of our study (76-week-old rats) we performed echocardiographic examination again. Heart rate did not differ significantly among the groups (CFY: 266±19, SHR-C: 269±22, SHR-L: 261±25). The long-term administration of L-2286 could not influence significantly the elevated blood pressure of SHR rats. The worst LV systolic functions (EF (%): CFY: 71.07±1.89, SHR-C^{76w}: 52.41±1.85, SHR-L^{76w}: 69.11±1.95, FS (%): CFY: 41.9±1.71, SHR-C^{76w}: 28.08±1.23, SHR-L^{76w}: 40.25±1.64) were found in the SHR-C group ($p<0.01$ vs. CFY and SHR-L). Although the systolic LV function was lower in the SHR-L group compared to the CFY group, this difference was not significant. LVEDD (left ventricular end diastolic diameter), LVESD (left ventricular end systolic diameter) were significantly enlarged in the SHR-C group compared to other groups ($p<0.01$). The lowest values among these above mentioned parameters were observed in the CFY group, but these values did not differ significantly from the SHR-L group.

The thickness of septum and PW was significantly elevated in the SHR groups, compared to the CFY group (PW: $p<0.05$, septum: $p<0.05$ vs. SHR-C group, and $p<0.01$ vs. SHR-L group). The left ventricular wall thickness (septum and PW) did not differ significantly between the two SHR groups. LV mass (uncorrected) was also increased in the SHR groups ($p<0.01$) compared to the CFY group, and L-2286 treatment decreased LV mass significantly ($p<0.01$) compared to the SHR-C group, similar to LV mass index (LV mass/body weight). Finally the significantly elevated RWT ($p<0.05$ SHR groups vs. CFY group) was not moderated by L-2286 administration (Table 5).

Time course change of blood pressure was measured by invasive method. The significantly elevated blood pressure of SHRs ($p<0.01$ CFY vs. SHR-C and SHR-L groups) was not influenced by L-2286 treatment. In healthy rats, blood pressure was also not affected by L-2286 administration (Fig. 13).

	CFY^{76w}	SHR-C^{76w}	SHR-L^{76w}
EF (%)	71.07±1.89	52.41±1.85^{a}	69.11±1.95
FS (%)	41.9±1.71	28.08±1.23^{a}	40.25±1.64
EDD (mm)	7.1±0.13	8.23±0.2^{a}	7.27±0.06^{d}
ESD (mm)	4.08±0.06	5.92±0.18^{a}	4.35±0.12^{d}
LVEDV (ml)	278.5±5.94	368.49±7.13^{a}	279.04±5.07^{d}
LVESV (ml)	86.03±11.37	175.41±12.29^{a}	86.18±6.58^{d}
PW (mm)	1.72±0.04	2.06±0.09^{b}	2.15±0.05^{a}
Septum (mm)	1.79±0.04	2.12±0.08^{b}	2.21±0.05^{a}
RWT	0.42±0.01	0.49±0.02^{b}	0.6±0.01^{a,c}
LV mass (uncorr., mg)	1002.33±53.47	1438.12±97.36^{a}	1273.63±41.76^{a,c}
LV mass /BW (mg/g)	2.51±0.06	3.94±0.21^{a}	3.48±0.13^{a,c}
SAP^{76w} (mmHg)	142±10	228±7^{a}	224±9^{a}
DAP^{76w} (mmHg)	97±5	173±9^{a}	168±8^{a}
MAP^{76w} (mmHg)	112±7	192±6^{a}	187±7^{a}

Table 5. L-2286 treatment influenced echocardiographic parameters in spontaneously hypertensive rats (SHR). CFY: normotensive age-matched control rats, n=7, SHR-C^{76w}: 76 week-old SHR control rats, n=7, SHR-L^{76w}: 76 week-old SHR treated with L-2286 for 46 weeks, n=26. EF: ejection fraction, FS: fractional shortening, EDD: end-diastolic diameter, ESD: end-systolic diameter, LVEDV: left ventricular (LV) end-diastolic volume, LVESV: LV end-systolic volume, Septum: thickness of septum, PW: thickness of posterior wall, RWT: relative wall thickness, LV mass: weight of LV, BW: body weight. SAP, DAP, MAP: systolic, diastolic and mean arterial blood pressure at 56-week-old age (n=3 from each group). Values are mean±S.E.M. $^{a}p<0.01$ (vs. CFY group), $^{b}p<0.05$ (vs CFY group), $^{c}<0.01$ (vs. SHR-C).

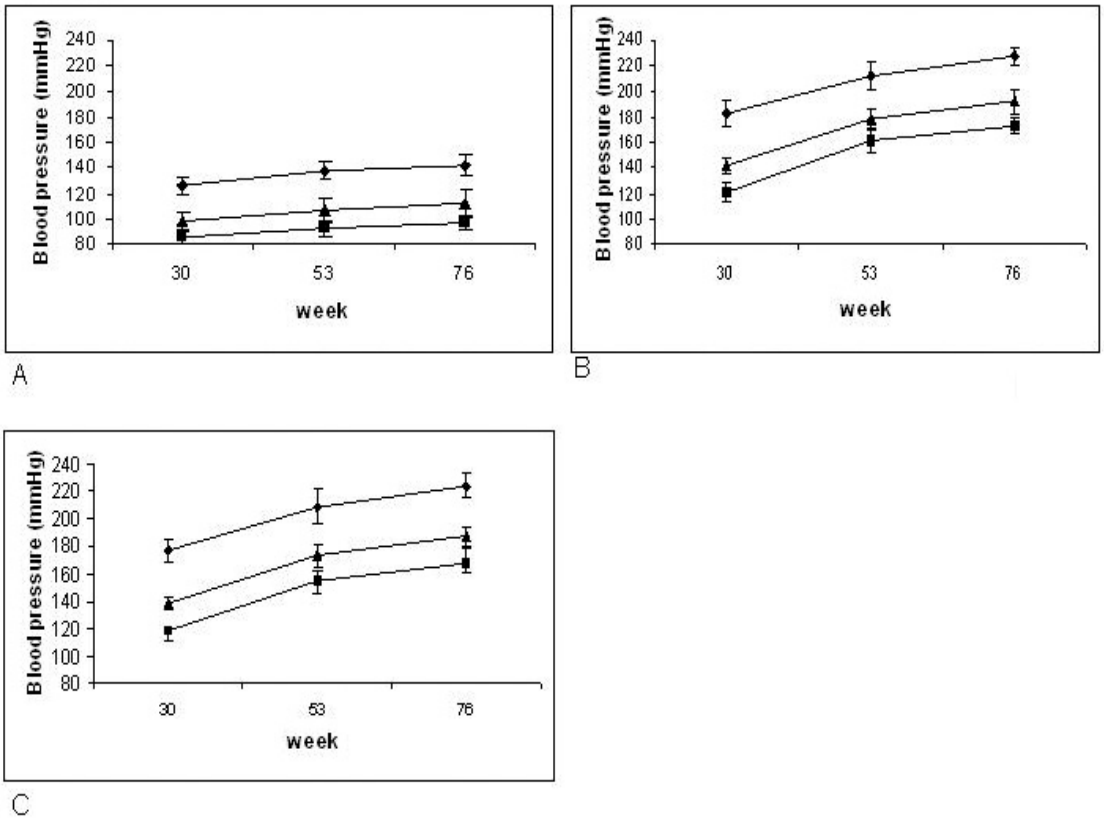

Figure 13. Effect of L-2286 treatment on blood pressure. A: CFY, normotensive control group, B: SHR-C: spontaneously hypertensive rats receiving only placebo, C: SHR-L: spontaneously hypertensive rats treated with L-2286 for 46 weeks. Values are means±SEM, n=5 from each group: ♦: systolic arterial blood pressure, ■: diastolic arterial blood pressure, ▲: mean arterial blood pressure.

6. Discussion

6.1. Cardioprotection by PARP inhibition in postinfarction heart failure model

Our study strengthened the previous data of our workgroup that an isoquinoline derivate PARP inhibitor had a very prominent protective effect against postinfarction myocardial remodeling in rats (19). However our recent work demonstrated firstly, that PARP inhibitors can activate the Akt-1/GSK-3β prosurvival signaling pathway, during postinfarction heart failure. We also compared the efficacy of complete PARP inhibition to that of complete ACE inhibition.

Our experimental compound L-2286 was tested in rats with failing heart following isoproterenol-induced myocardial infarction. As it is known, subcutaneous administration of the beta 1, 2-adrenoceptor agonist ISO produces generally patchy, particulary subendocardial myocardial cell death with replacement fibrosis, and impairs LV function, at least, partially, through free radical generation. Although the coronary vasculature remains intact, but ISO has positive chrono-, ino-, and dromotropic effects, so the oxygen and energy consumption of the myocardium will be substantially increased. ISO is rapidly metabolized by the monoamine oxidase and catechol-O-methyltransferase systems so chronic adverse effects of the drug can be avoided. The initial cell loss leads to consequent myocardial hypertrophy and ventricular enlargement (19, 22).

Several studies suggest that reactive oxygen species (ROS) and peroxynitrite contribute to the ischemia- and reperfusion-induced cardiac injury and initiate lipid peroxidation, protein oxidation, single-strand DNA breaks which can activate the nuclear poly(ADP-ribose)polymerase (PARP). Our previous data showed that PARP inhibitors were able to reduce the oxidative damage of cellular components (5, 19). It was showed that PARP was activated in the reperfused myocardium in animals (23) and recently it was also proven in human failing heart samples (24). It was also proven that ROS-induced oxidative damages and PARP activation represent an important mechanism of the pathological processes in postischemic HF (25).

On the other hand, ACE-inhibitors are widely used drugs in the treatment of HF. In HF the elevated level of circulating angiotensin II (Ang II) is the main effector of the

activated renin-angiotensin system (RAS) and increased sympathetic activity, and causes a vicious circle.

Cardiac remodeling is characterized by inadequate myocyte hypertrophy and accumulation of extracellular matrix structural proteins (fibrillar collagen, type I and III collagen), which cause myocardial stiffness and adversely affect myocardial viscoelasticity, ultimately leading to diastolic and systolic dysfunctions (25). Our results showed, that both PARP- and ACE- inhibition exerted beneficial effect on the progression of postinfarction myocardial remodeling characterized by ventricular hypertrophy and interstitial fibrosis, which is in accordance with other studies (19, 26). PARP-inhibitor L-2286 had significantly greater protective effect against postinfarction remodeling, than enalapril.

Previous works demonstrated that PARP-inhibitors induced the phosphorylation and activation of Akt-1 in several organs and also in reperfused myocardium, raising the possibility that protective effect of PARP-inhibition can be mediated through the phosphatidylinositol 3-kinase (PI3K)/Akt pathway (5). Accumulated data suggest that PI3K/Akt signaling tranduces adaptive cardiac hypertrophy and constitutive activation of cardiomyocytes by PI3K/Akt activation did not transit into a maladaptive hypertrophy. ACE inhibitor also influenced the activity of Akt-1 (26). Our recent work showed, that the phosphorylation of Akt-1^{Ser473} was elevated in ISO-treated group, and both PARP-inhibiton and ACE-inhibition caused a further growth of it. The PARP-inhibitor L-2286 caused a significantly greater activation of Akt-1, compared to enalapril. In our experiment the phosphorylation (therefore the inhibition) of GSK-3β^{Ser9} was the highest in the L-2286 treated group. Enalapril exerted a significantly less inhibition of GSK-3β^{Ser9}.

The MAPKs ERK, JNK, and p38 can all be activated by AngII (27). The exact role of MAPKs is still controversial in CHF. The moderate phosphorylation of ERK1/2$^{Thr183-Tyr185}$ was further attenuated by ISO and became more elevated by other treatments. It was reported that ERK 1/2 activation leads to a concentric form of hypertrophy with enhanced cardiac function (19) and MEK1-ERK2 protects the heart from ischemia induced apoptotic insults in mices (25). In our study the ISO-treated group p38 MAPK$^{Thr180-Gly-Tyr182}$ was slightly phosphorylated, while all other treatments increased the

phosphorylation of p38-MAPK$^{Thr180\text{-}Gly\text{-}Tyr182}$ significantly. Whereas myocyte apoptosis and growth are attributable to activation of p38-α, p38-β activation appears to mediate a survival pathway, involving promotion of myocyte growth and reduction of apoptosis (28). Because our antibody recognized both the above mentioned isoforms of p38-MAPK and no information is available regarding the relative abudance of p38α and p38β MAPK in rat heart, and the phosphorylation state was also significant in control rats, the favorable effect of these treatments tends to suggest that p38β MAPK is a predominant isoform activated in this rodent heart (29). In case of JNK, ISO significantly decreased its phosphorylation and both L-2286 and E treatment augmented its activation. JNK activation was observed in the failing human heart and active JNK is associated with oxidative stress and myocyte apoptosis after large MI in rats (30).

It has been reported that PKC expression is increased in cardiac hypertrophy induced by pressure-overload in rats. It was reported that L-2286 can slow the progression of cardiac hypertrophy into heart failure partially by promoting GSK-3β activity via interruption of upstream PKC signaling (19). The phosphorylation of PKC pan βII^{Ser660} and PKC α/βII$^{Thr638/641}$ increased after ISO-induced MI, however their phosphorylation decreased upon administering ACE or a PARP-inhibitor. The PARP-inhibitor - L-2286 decreased the activity of the prohypertrophic PKC α/β more effectively than the ACE-inhibitor – enalapril. A very similar phosphorylation pattern was revealed in the case of PKCδ Thr^{505} and PKC ζ/λ Thr$^{410/403}$.

PKC-ε^{Ser729} is activated by various types of stress. It was demonstrated that PKC-ε forms a signalling complex and acts co-operatively with Akt-1 to protect human vascular endothelial cells against apoptosis (31). Preischemic application of landiolol, a highly selective β1-blocker, induces cardioprotective effects through PKC-ε-mediated pathway in Langendorff-perfused rat hearts (32). In our study we detected a positive effect (activation) of PARP inhibitor on PKC-ε^{Ser729}, which is responsible for adaptive changes in stress situations, while the levels of other PKC (-α, -β, -ζ, -δ) isoforms were reduced, which are responsible for maladaptive myocardial hypertrophy and remodeling in postinfarction animals.

In postinfarction model echocardiographic parameters - systolic LV function, wall thickness, LVESV, LVEDV - worsened in ISO-group compared to control animals. This

effect can be due to the evolved myocardial fibrosis and cardiomyocyte hypertrophy and partially due to the activation of sevaral protein kinases (e.g. PKC-α/βII$^{Thr638/641}$). Enalapril treatment decreased significantly this worsening, however PARP-inhibitor treatment could nearly completely prevent it. Interestingly, the LVEDV was unchanged despite the ACE-inhibitor, or PARP-inhibitor treatment. The underlying mechanism whereby the PARP-inhibitor L-2286 can exert this favourable effect, is its activator effect on several prosurvival (especially Akt-1-GSK 3β, PKC-ε) and inhibitor effect on prohypertrophic (PKC- α/β, - ζ/λ, -δ) protein kinases.

6.2. Effect of long-term L-2286 administration on hypertension induced heart failure

The major findings of this study are that chronic inhibition of nuclear PARP enzyme reduces ADP-ribosylation of nuclear proteins and thus prevents the development of HF from cardiac hypertrophy with inducing reverse remodeling with restoration of cardiac structure and function while changing the altered patterns of signal transducting processes. We used the SHR which provides an animal model of high blood pressure that is similar to essential hypertension in humans (50). They are characterized by the fact that they suffer from pre-hypertension (systolic blood pressure (SBP) 100-120 mm Hg) during the first 6-8 weeks of their life, and develop sustained hypertension over the next 12-14 weeks (37). Our study began in the compensated phase of hypertensive cardiopathy in SHR with signs of LVH (at 30-week-old) and after 46 weeks the obvious signs of HF could be detected in SHRs. The development of HF from long-term hypertension can be explained by different mechanism in the literature (43, 44), but oxidative stress and abnormal signalings are generally respected as the molecular basis of the disease (3, 45, 46).

In the case of ischemia-reperfusion induced cardiac damages and PARP activation is respected as one of the main mechanisms of the damage of cardiomyocytes, it is well-documented- that PARP inhibitors have beneficial effects. However, in case of long-term hypertension induced cardiac hypertrophy followed by HF, there is no data available about the possible role of PARP. Furthermore, our previous works demonstrated, that inhibition of PARP has a major effect on signalling in oxidative stress in cardiomyocytes

(5), by activating the PI-3-kinase-Akt pathway and inhibiting JNK and p38 MAP kinases (47). One of the PARP inhibitors used in our previous studies was L-2286 which had a protective effect in ischemia-reperfusion injury (18) and in isoproterenol induced cardiac remodeling (19) without having any detectable side effects in animal models. In this study, we tested the effect of PARP inhibition in aging SHRs having cardiac hypertrophy and fibrosis related to higher mechanical and oxidative stress and had typical signs of HF (gravimetric parameters, observation daily) and impaired systolic LV function. These conditions have important role in the pathogenesis of diastolic and systolic dysfunctions in hypertensive heart disease (30).

Both in animal models and in humans, increased blood pressure has been associated with oxidative stress in the vasculature, i.e. with an excessive endothelial production of ROS, which may be both a cause and a consequence of hypertension (50). ROS-induced DNA damages can lead to the activation of PARP enzyme. The effect of PARP-inhibitors on oxidative stress has been investigated in several studies (1, 18, 53). In our experiment PARP-inhibitor administration did not influence the elevated blood pressure in SHRs, just like in human studies, where the use of antioxidants had only limited effects on hypertension or cardiovascular endpoints (50). Therefore, although SHR is an increased afterload model of hypertension, in this study, the observed beneficial alterations can not be explained by a blood pressure lowering effect. Chronic untreated hypertension often leads to excessive collagen deposition as part of the process of cardiovascular remodeling that includes LVH and endothelial dysfunction. This remodeling leads to a more rigid myocardium and ultimately to HF with impaired diastolic and systolic LV function. In our experiment the level of plasma-BNP was elevated in both SHR groups and this finding was similar to de Bold's (55), who examined the mRNA level of plasma BNP in SHR rats at different ages. Exalted BNP production and release by cardiocytes occurs in hypertension and has been considered to be a compensatory mechanism against ventricular overload (55). The Framingham study demonstrated that an increase in BNP predicted the risk of death and cardiovascular events (56). This alteration could be mitigated by PARP-inhibition and in accordance with this, the survival rate of treated rats was also significantly better. If the heart experiences extended periods of elevated workload, it undergoes a hypertrophic enlargement in response to increased demand. A

number of signalling modulators in the vasculature milieu are known to regulate heart muscle mass, including those that influence gene expression, apoptosis, cytokine release and growth factor signaling (49). One of them is the Akt-1-GSK-3β pathway, which was favorably influenced by PARP inhibitor. In our experiment the down-regulated phosphorylation of Akt-1/GSK-3β in SHR-C samples were increased by PARP inhibitor. Similar effects of PARP inhibition were seen in different experimental systems indicating that Akt activation is an important step in the cytoprotective effects of PARP inhibition (5, 6). Akt-1 is well known to play a central role in the development of physiologic hypertrophy, but also has an important role in cardiac angiogenesis through the activation of mammalian target of rapamycin (mTOR). It is likely that ineffective angiogenesis might contribute to the transition from LVH to HF (9). The protecting effect of PARP-inhibitors against the development of HF from LVH can be mediated at least partly through the Akt-1/mTOR signaling. MAPKs are ubiquitously expressed, and their specific functions in the heart have been a focus of intensive study (39). Growing evidence suggests, that modulation of the complex network of MAPKs cascades could be a rewarding approach to the treatment of cardiomyocyte hypertrophy and HF (9). In our experiment the elevated activation of p38, JNK in the SHR-C groups were decreased, while the activation of ERK was increased by L-2286. While the ERKs are particularly implicated in growth-associated responses, the p38 MAPK and JNKs are generally activated by cytotoxic stress factors (9).

JNK directly phosphorylates the pro-apoptotic factor Bad, enhancing cell death through the intrinsic pathway. Qin et al. found, that the increase in p38 activity was associated with increased oxidative stress in the remote noninfarcted myocardium after myocardial infarction (MI) (30). In vivo, a number of reports have shown protection from ischemia-induced apoptosis and cardiac dysfunction through the acute use of p38 inhibitors (52). Activation of ERK causes cardiac hypertrophy and increases survival, while inactivation of ERK contributes to myocyte apoptosis (30). Cardiac-specific expression of constitutively activated MEK1 promotes cardiac hypertrophy without compromised function or long-term animal survival, suggesting that activation of ERK activity promotes a compensated form of hypertrophy (39). There is now considerable evidence,

that a variety of PKC isoforms also act as major modulators of the myocyte death machinery, having both pro and anti-apoptotic effects.

In our study, the phosphorylation of PKC pan βII^{Ser660}, $\alpha/\beta IIThr^{638/641}$, δ^{Thr505} and $\zeta/\lambda^{Thr410/403}$ were attenuated in SHR-L compared to SHR-C by PARP inhibitor. Several reports suggest, that PKC α and β are involved in the development of cardiac hypertrophy and HF (8). PKC α and β are increased in the failing human heart due to dilated and ischemic cardiomyopathy (51). Activation of PKC δ appears to contribute to ischemic injury in cardiac myocytes (52). Koide et al. revealed that PKC α, β and δ were up-regulated from the stage of cardiac hypertrophy extending to congestive HF (8). The hypothesis that PKC δ is pro-apoptotic while PKC ε is anti-apoptotic is also supported by a number of in vivo reports (8, 52). The activation of PKC ε was upregulated by L-2286 treatment in SHR-L group. In this experiment, there were no differences in LV systolic functions (EF, FS) at baseline (the age of 30 weeks). These parameters were preserved in the CFY and SHR-L groups, but moderated in the SHR-C group at the end of the study. L-2286 increased EF by reducing end-systolic dimensions (3). During the development of hypertension, alterations in LV geometry may occur as an adaptation to increasing pressure and volume load. In hypertensive patients, LV geometry can be classified into four patterns on the basis of LV mass index and RWT (41). In conformity with this classification eccentric hypertrophy was found in SHR-C group (increased LV mass/ BW and normal RWT), while L-2286 administration could preserve concentric hypertrophy (increased LV mass/ BW and increased RWT) state, which could be detected at the beginning of the study in both SHR groups. Therefore, the ineffectiveness of L-2286 on thickness of septum and PW can be considered as a favorable effect because it can add to the maintaining of concentric hypertrophy.

7. Summary

Throughout the last 2 decades, experimental evidences from in vitro studies and preclinical models of diseases have demonstrated that reactive oxygen and nitrogen species, including reactive oxidant peroxynitrite, are generated in parenchyma, endothelial, and infiltrating inflammatory cells during myocardial and other forms of reperfusion injury, myocardial hypertrophy, heart failure, cardiomyopathies and cardiovascular aging. In related animal models of diseases, pharmacological inhibition of PARP provides significant therapeutic benefits. Therefore, novel antioxidants and PARP inhibitors have entered into the clinical development for the experimental therapy of various cardiovascular and other diseases (53).

In our experiments, the common feature of the PARP-inhibitor L-2286 treatment was the beneficial action on several intracellular signaling pathways PI-3-kinase-Akt-1^{Ser473} and PKC ε^{Ser729} pathways, it can influence favorably the gravimetric and echocardiographic parameters and cardiac fibrosis. In addition, in our last investigation (HF model), L-2286 treatment could delay the onset of hypertension-induced HF.

8. Acknowledgements

These studies were carried out at the Department of Biochemistry and Medical Chemistry and at the Ist Department of Medicine, Medical School of the University of Pécs between 2005 and 2008.

I would like to express my thanks to my teacher and program leader, Professor Kálmán Tóth, who managed my studies and gave a support and useful advises during my work.

I am grateful to Professor Balázs Sümegi who taught me a biochemical way of thinking. He directed my work on the field of PARP inhibitors and he ensured the possibility of undisturbed work in his department for me.

I am really thankful to Professor Kálmán Hideg who taught me enthusiastic on free radical mediated processes and directed my work on the field of cardioprotective effects of PARP inhibitor compounds.

I convey my thanks to Robert Halmosi for his excellent work and help to perform echocardiographic examinations.

Dr. Habon Tamás, Dr. Eszter Szabados, Izabella Solti, Dr. N. Kiss Gyöngyi, Eniko Plozer, Alíz Szabó, Dr. László Kereskai and Dr. Endre Kálmán gave a hand with a part of the experiments. I am grateful to Istvánné Pásztor, Heléna Halász, Bertalan Horváth and László Girán, who gave much assitance in the laboratory work.

I express my gratitude and thanks to my friends for their encouraging support during my studies and work.

9. References:

1. Pacher P, Szabó C. Role of poly(ADP-)ribose polymerase 1 (PARP-1) in cardiovascular diseases: the therapeutic potential of PARP inhibitors. Cardiovasc Drug Rev 2007;25:235-260.

2. Graziani G, Szabó C. Clinical perspectives of PARP inhibitors. Pharmacol Res 2005;52:109-118.

3. Moens AL, Takimoto E, Tocchetti CG, Chakir K, Bedja D, Cormaci G, Ketner EA, Biswal S, Channon KM, Wolin MS, Alp NJ, Paolocci N, Champion HC, Kass DA. Reversal of cardiac hypertrophy and fibrosis from pressure overload by tetrahydrobiopterin: efficacy of recoupling nitric oxide synthase as a therapeutic strategy. Circulation 2008;117:2626-2636.

4. Szabó C, Pacher P, Zsengellér Zs, Vaslin A, Komjáti K, R. Benkő, Chen M, Mabley JG, Kollai M. Angiotensin II-mediated endothelial dysfunction: role of poly(ADP-ribose)polymerase activation. Mol Med 2004;10:28-35.

5. Tapodi A, Debreceni B, Hanto K, Bognar Z, Wittmann I, Gallyas F Jr, Varbiro G, Sumegi B. Pivotal role of Akt activation in mitochondrial protection and cell survival by poly(ADP-ribose)polymerase-1 inhibition in oxidative stress. J Biol Chem 2005;280:35757-35775.

6. Kovacs K, Toth A, Deres P, Kalai T, Hideg K, Gallyas F Jr, Sumegi B. Critical role of PI3-kinase/Akt activation in the PARP inhibitor induced heart function recovery during ischemia-reperfusion. Biochem Pharmacol 2006;71:441-452.

7. Bogoyevitch MA. Signalling via stress-activated mitogen-activated protein kinases in the cardiovascular system. Cardiovasc Res 2000;45:826-842.

8. Koide Y, Tamura K, Suzuki A, Kitamura K, Yokoyama K, Hashimoto T, hirawa N, Kihara M, Ohno S, Umemura S. Differential induction of protein kinase C isoforms at the cardiac hypertrophy stage and congestive heart failure stage in Dahl Salt-Sensitive rats. Hypertens Res 2003;26:421-426.

9. Luedde M, Katus HA, Frey N. Novel molecular tergets in the treatment of cardiac hypertrophy. Recent Patents on Cardiovasc Drug Discov 2006,1:1-20.

10. Teerlink JR, Pfeffer JM, Pfeffer MA. Progressive ventricular remodeling in response to diffuse isoproterenol-induced myocardial necrosis in rats. Circ Res 1994;75:105-113.
11. Zhang GX, Kimura S, Nishiyima A, Shokoji T, Rahman M, Yao L, Nagai Y, Fujisawa Y, Miyatake A, Abe Y. Cardiac oxidative stress in acute and chronic isoproterenol-infused rats. Cardiovasc Res 2005;65:230-238.
12. Grimm D, Elsner D, Schunkert H, Pfeifer M, Griese D, Bruckschegel G, Muders F, Riegger GAJ, Kromer EP. Development of heart failure following isoproterenol administration in the rat: role of the renin-angiotensin system. Cardiovasc Res 1998;37:91-100.
13. van Eickels M, Schreckenberg R, Doevendans PA, Meyer R, Grohé C, Schlüter KD. The influence of oestrogen-deficiency and ACE inhibition on the progression of myocardial hypertrophy in spontaneously hypertensive rats. Eur J Heart Fail 2005,7:1079-1084.
14. Meurrens K, Ruf S, Ross G, Schleef R, von Holt K, Schlüter KD. Smoking accelerates the progression of hypertension-induced myocardial hypertrophy to heart failure in spontaneously hypertensive rats. Cardiovasc Res 2007;76:311-322.
15. McCrossan ZA, Billeter R, White E. Transmural changes in size, contractile and electrical properties of SHR left ventricular myocytes during compensated hypertrophy. Cardiovasc Res 2004;63:283-292.
16. Kulcsár Gy, Kálai T, Ősz E, Sár CP, Jekő J, Sumegi B, et al. Synthesis and study of new 4-quinazolinone inhibitors of the DNA repair enzyme poly(ADP-ribose) polymerase (PARP). Arkivoc 2006;IV:121-131.
17. Hideg K, Kálai T, Sümegi B. Quinazoline derivates and their use for preparation of pharmaceutical compositions having PARP-Enzyme inhibitory effect. 2003;WO2004/096779, Hung. Pat. PO301173.
18. Palfi A, Toth A, Kulcsár Gy, Hanto K, Deres P, Bartha E, et al. The role of Akt and mitogen-activated protein kinase systems in the protective effect of poly(ADP-ribose)polymerase inhibition in Langendorff perfused and in isoproterenol-damaged hearts. J Pharmacol Exp Ther 2005;315:273-282.

19. Palfi A, Toth A, Hanto K, Deres P, Szabados E, Szereday Z, et al. PARP inhibition prevents postinfarction myocardial remodeling and heart failure via protein kinase C/glygogen synthase kinase-3β pathway. J Mol Cell Cardiol 2006;41:149-159.
20. Haddad GE, Coleman BR, Zhao A, Blackwell KN (2005) Regulation of atrial contraction by PKA and PKC during development and regression of eccentric cardiac hypertrophy. Am J Physiol Heart Circ Physiol 2005;288:H695-704.
21. Koide Y, Tamura K, Suzuki A, Kitamura K, Yokoyama K, Hashimoto T, et al. Differential induction of protein kinase C isoforms at the cardiac hypertrophy stage and congestive heart failure stage in Dahl Salt-Sensitive rats. Hypertens Res 2003;26:421-25.
22. Teerlink JR, Pfeffer JM, Pfeffer MA. Progressive ventricular remodeling in response to diffuse isoproterenol-induced myocardial necrosis in rats. Circ Res 1994;75:105-113.
23. Halmosi R, Berente Z, Osz E, Toth K, Literati-Nagy P, Sumegi B. Effect of poly(ADP-ribose) polymerase inhibitors on the ischemia-reperfusion-induced oxidative cell damage and mitochondrial metabolism in Langendorff heart perfusion system. Mol Pharmacol 2001;59:1497-1505.
24. Molnár A, Tóth A, Bagi Zs, Papp Z, Édes I, Vaszily M, et al. Activation of the poly(ADP-ribose)polymerase pathway in human heart failure. Mol Med 2006;12:143-152.
25. Lips DJ, Bueno OF, Wilkins BJ, Purcell NH, Kaiser RA, Lorenz JN, et al. MEK1-ERK2 Signaling pathway protects myocardium from ischemic injury in vivo. Circulation 2004;109:1938-1941.
26. Grimm D, Elsner D, Schunkert H, Pfeifer M, Griese D, Bruckshlegel G, et al. Development of heart failure following isoproterenol administration in the rat: role of the renin-angiotensin system. Cardiovasc Res 1998;37:91-100.
27. Penela P, Murga C, Ribas C, Tutor SA, Peregrin S, Mayor F Jr. Mechanisms of regulation of G protein-coupled receptor kinases (GRKs) and cardiovascular disease. Cardiovasc Res 2006;69:46-56.
28. See F, Thomas W, Way K, Tzanidis A, Kompa A, Lewis D, et al. p38 Mitogen-Activated protein kinase inhibition improves cardiac function and attenuates left ventricular remodeling following myocardial infarction in the rat. J Am Coll Cardiol 2004;44:1679-89.

29. Kyoi S, Otani H, Matsuhisa S, Akita Y, Tatsumi K, Enoki C, et al. Opposing effect of p38 MAP kinase and JNK inhibitors on the development of heart failure in the cardiomyopathic hamster. Cardiovasc Res 2006;69:888-898.

30. Qin F, Liang MC, Liang C-S. Progressive left ventricular remodeling, myocyte apoptosis, and protein signaling cascades after myocardial infarction in rabbits. Biochim Biophys Acta 2005;1740:499-513.

31. Steinberg R, Harari OA, Lidington EA, Boyle JJ, Nohadani M, Samarel AM, et al. A protein kinase Cepsilon/anti-apoptotic kinase signalling complex protects human vascular endothelial cell against apoptosis through induction of Bcl-2. J Biol Chem 2007;282:32288-32297.

32. Takeishi Y, Bhagwat A, Ball AN, Kirkpatrick DL, Periasamy M, Walsh RA. Effect of angiotensin-converting enzyme inhibition on protein kinase C and SR protein in heart failure. Am J Physiol 1999;276:H53-62.

33. de Bold MLK. Atrial Natriuretic factor and brain natriuretic peptide gene expression in the spontaneously hypertensive rat during postnatal development. Am J Hypertens 1998;11:1006-1018.

34. Nishikimi T, Maeda N, Matsuoka H. The role of natriuretic peptides in cardioprotection. Cardiovasc Res 2006;69:318-28. Review

35. Wei SG, Yu Y, Zhang ZH, Weiss RM, Felder RB. Angiotensin II-triggered p44/42 mitogen-activated protein kinase mediates sympathetic excitation in heart failure rats. Hypertension 2008;52:342-350.

36. Taniike M, Yamaguchi O, Tsujimoto I, Hikoso S, Takeda T, Nakai A, Omiya S, Mizote I, Nakano Y, Higuchi Y, Matsumura Y, Nishida K, Ichijo H, Hori M, Otsu K. Apoptosis signal-regulating kinase 1/p38 signaling pathway regulates physiological hypertrophy. Circulation 2008;117:545-52.

37. Li HH, Willis MS, Lockyer P, Miller N, MCDonough H, Glass DJ, Patterson C. Atrogin-1 inhibits Akt-dependent cardiac hypertrophy in mice via ubiquitin-dependent coactivation of Forkhead proteins. J Clin Invest 2007;117:3211-23.

38. Ni YG, Berenji K, Wang N, Oh M, Sachan N, Dey A, Cheng J, Lu G, Morris DJ, Castrillon DH, Gerard RD, Rothermel BA, Hill JA. Foxo transcription factors blunt cardiac hypertrophy by inhibiting calcineurin signaling. Circulation 2006;114:1159-1168.

39. Wang Y. Mitogen-Activated Protein Kinases in heart development and diseases. Circulation 2007;116:1413-1423.Review
40. Wang J, Liu X, Sentex E, Takeda N, Dhalla NS. Increased expression of protein kinase C isoforms in heart failure due to myocardial infarction. Am J Physiol Heart Circ Physiol 2003;284:H2277-2287.
41. Kokubo M, Uemura A, Matsubara T, Murohara T. Noninvasive evaluation of the time course of change in cardiac function in spontaneously hypertensive rats by echocardiography. Hypertens Res 2005;7:601-9.
42. Ito N, Ohishi M, Yamamoto K, Tatara Y, Shiota A, Hayashi N, Komai N, Yanagitani Y, Rakugi H, Ogihara T. Renin-Angiotensin inhibition reverses advanced cardiac remodeling in aging spontaneously hypertensive rats. Am J Hypertens 2007;20:792-799.
43. Palaniyandi SS, Inagaki K, Mochly-Rosen D. Mast cells and epsilon PKC: A role in cardiac remodeling in hypertension-induced heart failure. J Mol Cell Cardiol 2008;45:779-786.
44. Wei SG, Yu Y, Zhang ZH, Weiss RM, Felder RB. Angiotensin II-triggered p44/42 mitogen-activated protein kinase mediates sympathetic excitation in heart failure rats. Hypertension 2008;52:342-350.
45. Monti J, Fischer J, Paskas S, Heinig M, Schulz H, Gösele C, Heuser A, Fischer R, Schmidt C, Schirdewan A, Gross V, Hummel O, Maatz H, Patone G, Saar K, Vingron M, Weldon SM, Lindpainter K, Hammock BD, Rohde K, Dietz R, Cook SA, Schunk WH, Luft FC, Hubner N. Soluble epoxide hydrolase is a susceptibility factor for heart failure in rat model of human disease. Nat Genet 2008;40:529-537.
46. Nishio M, Sakata Y, Mano T, Yoshida J, Ohtani T, Takeda Y, Miwa T, Masuyama T, Yamammoto K, Hori MJ. Therapeutic effects of angiotensin II type receptor blocker at advanced stage of hypertensive diastolic heart failure. J Hypertension 2007;25:455-461.
47. Veres B, Radnai B, Gallyas F Jr, Varbiro G, Berente Z, Osz E, Sumegi B. Regulation of kinase cascades and transcription factors by a poly(ADP-ribose)polymerase-1 inhibitor, 4-hydroxyquinasoline, in lipopolysaccharide-induced inflammation in mice. J Pharmacol Exp Ther 2004;310:247-255.

48. Inagaki K, Koyanagi T, Berry NC, Sun L, Mochly-Rosen D. Pharmacological inhibition of ε-Protein Kinase C attenuates cardiac fibrosis and dysfunction in hypertension-induced heart failure. Hypertension 2008;51:1565-1569.
49. Barry SP, Davidson SM, Townsend PA. Molecular regulation of cardiac hypertrophy. Int J Biochem Cell Biol 2008;40:2023-2039.
50. Puddu P, Puddu GM, Cravero E, Rosati M, Muscari A. The molecular sources of reactive oxygen species in hypertension. Blood Press 2008;17:70-77.
51. Bowling N, Walsh RA, Song G, Estridge T, Sandusky GE, Fouts RL, Mintze K, Pickard T, Roden R, Bristow MR, Sabbah HN, Mizrahi JL, Gromo G, King GL, Vlahos CJ. Increased protein kinase C activity and expression of Ca^{2+}-sensitive isoforms in the failing human heart. Circulation 1999;99:384-391.
52. Baines CP, Molketin JD. STRESS signaling pathways that modulate cardiac myocyte apoptosis. J Mol Cell Cardiol 2005;38:47-62.
53. Pacher P, Szabo C. Role of the peroxynitrite-poly(ADP-ribose)polymerase pathway in human disease. Am J Pathol 2008;173:2-13.
54. López N, Varo N, Díez J, Fortuño MA. Loss of myocardial LIF recepor in experimental heart failure reduces cardiotrophin-1 cytoprotection. A role for neurohormonal agonists? Cardiovasc Res 2007;75:536-545.
55. de Bold MLK. Atrial Natriuretic factor and brain natriuretic peptide gene expression in the spontaneously hypertensive rat during postnatal development. Am J Hypertens 1998;11:1006-1018.
56. Seki S, Tsurusaki T, Kasai T, Taniguchi I, Mochizuki S, Yoshimura M. Clinical significance of B-type natriuretic peptide in the assasment of untreated hypertension. Circ J 2008;72:770-777.
57. Miura T, Miki T. GSK-3β, a therapeutic target for cardiomyocyte protection. Circ J 2009;73:1184-1192. Review.
58. Webster KA, Graham RM, Thompson JW, Spiga M-G, Fraizer DP, Wilson A, Bishopric. Redox stress and the contributions of BH3-only protein to infarction. Antioxid Redox Signal 2006;8:1667-1676. Review.
59. Hori M, Nishida K. Oxidative stress and left ventricular remodelling after myocardial infarction. Cardiovasc Res 2009;81:457-464.

60. Bing OHL, Conrad CH, Boluyt MO, Robinson KG, Brooks WW. Studies of prevention, treatment and mechanisms of heart failure in the aging spontaneously hypertensive rat. Heart Fail Rev 2002;7:71-88.
61. Zhang Y-W, Shi J, Li Y-J, Wei L. Cardiomyocyte death in doxorubicin-induced cardiotoxicity. Arch Immunol Ther Exp 2009;57:435-445. Review
62. Boluyt MO, Bing OHL. Matrix gene expression and decompensated heart failure: The aged SHR model. Cardiovasc Res 2000;46:239-249. Review.
63. Paton JFR, Wang S, Polson JW, Kasparov S. Signalling across the blood brain barrier by angiotensin II: novel implications for neurogenic hypertension. J Mol Med 2008;86:705-710. Review.

10. Publications of the author

PALFI A, TOTH A, KULCSAR G, HANTO K, DERES P, BARTHA E, HALMOSI R, SZABADOS E, CZOPF L, KALAI T, HIDEG K, SUMEGI B, TOTH K. The role of Akt and MAP kinase systems in the protective effect of PARP inhibition in Langendorff perfused and in isoproterenol damaged rat hearts. J Pharmacol Exp Ther 2005; 315:273-82. (IF: 4.335)

BARTHA E, KISS GN, KALMAN E, KULCSÁR G, KALAI T, HIDEG K, HABON T, SUMEGI B, TOTH K, HALMOSI R. Effect of L-2286, a poly(ADP-ribose)polymerase inhibitor and enalapril on myocardial remodeling and heart failure. J Cardiovasc Pharmacol 2008; 52:253-61. (IF: 2.023)

BARTHA E, SOLTI I, KERESKAI L, LANTOS J, PLOZER E, MAGYAR K, SZABADOS E, KALAI T, HIDEG K, HALMOSI R, SUMEGI B, TOTH K. PARP inhibition delays transition of hypertensive cardiopathy to heart failure in spontaneously hypertensive rats. Cardiovasc Res 2009; 83:501-510. (IF: 5.947)

PALFI A, BARTHA E, CZOPF L, MARK L, GALLYAS F Jr, VERES B, KALMAN E, PAJOR L, TOTH K, OHMACHT R, SUMEGI B. Alcohol-free red wine inhibits isoproterenol-induced cardiac remodeling in rats by the regulation of Akt1 and protein kinase C alpha/beta II. J Nutr Biochem 2009; 6:418-425. (IF: 4.352)

Published abstracts

GY N KISS, P DERES, K HANTO, E BOGNAR, E BARTHA, B SUMEGI, Z BERENTE: Do PARP inhibitors affect myocardial metabolism? Barcelona, Spain, Annual Congress of European Society of Cardiology and World Congress of Cardiology, Sep 2-6., 2006, Barcelona, Spain. Abstract book 199.

BARTHA E, PALFI A, MARK L, KISS GN, HALMOSI R, SZABADOS E, KALMAN E, TOTH K, SUMEGI B. Effect of alcohol-free red wine extract on isoproterenol induced cardiac remodeling in rats. Pecs, Hungary, Vth Congress of International Symposium on Myocardial Cytoprotection, Sept 27-30, 2006, Pécs, Hungary.

BARTHA É, PÁLFI A, MÁRK L, KISS GN, HALMOSI R, SZABADOS E, SÜMEGI B. Alkoholmentes vörösbor-kivonat hatása az isoproterenol által kiváltott miokardiális remodellingre és egészséges patkányszívre. Magyar Kardiológusok Társasága 2007. évi Tudományos Kongresszusa, 2007. május 9-12., Balatonfüred, Card. Hung. Suppl. A, 2007; 37:A34.

HALMOSI R, BARTHA É, PÁLFI A, KÁLMÁN E, HIDEG K, SÜMEGI B, TÓTH K. PARP-gátlók és ACE-inhibitorok hatása az isoproterenol-indukálta szívelégtelenség progressziójára. Magyar Kardiológusok Társasága 2007. évi Tudományos Kongresszusa, 2007. május 9-12., Balatonfüred, Card. Hung. Suppl. A, 2007; 37:A17.

E BARTHA, R HALMOSI, GY Kulcsár, GY N KISS, E KALMAN, B SUMEGI, T KÁLAI, K HIDEG, K Toth: Effect of PARP inhibitors and ACE inhibitors on the progression of isoproterenol-induced heart failure. Annual Congress of European Society of Cardiology, Sept 1-5, 2007, Vienna, Austria. Abstract book 59.

BARTHA É, HALMOSI R, SOLTI I, PÁLFI A, KÁLMÁN E, SÜMEGI B, KÁLAI T, HIDEG K, TÓTH K. PARP- és ACE-gátlók kedvező hatása az isoproterenol-indukálta szívelégtelenség progressziójára. Magyar Szabadgyök Kutató Társaság IV. Kongresszusa, 2007. október 11-13., Pécs, Folia Hepatologica Suppl. 3, 2008:11:10.

BARTHA É, MAGYAR K, SOLTI I, KOVÁCS K, HIDEG K, SÜMEGI B, HALMOSI R, TÓTH K. Poli(ADP-ribóz)polimeráz enzim gátlásának hatása fiatal spontán hipertenzív patkány szívekre. Magyar Kardiológusok Társasága 2008. évi Tudományos Kongresszusa, 2008. május 7-10., Balatonfüred, Card. Hung. Suppl. B, 2008; 38:B8.

E. BOGNAR, GY. N. KISS, ZS. SARSZEGI, E. BARTHA, I. SOLTI, B. SUMEGI, Z. BERENTE. Poly(ADP-ribose)Polymerase (PARP) inhibitor HO3089 enhanced post ischemic, myocardial glucose uptake mostly by activation of AMP-activated protein kinase (AMPK)., World Congress of Cardiology 2008, May 18-21., 2008, Buenos Aires, Argentina. Circulation 2008; e162-e413, 73, P410.

E. BARTHA, R. HALMOSI, I. SOLTI, E. BOGNAR, K. KOVACS, T. HABON, T. KÁLAI, B. SUMEGI, K. HIDEG, K. TOTH. Effect of PARP inhibition on young spontaneously hypertensive rat (SHR) hearts. Buenos Aires, Argentina, World Congress of Cardiology 2008, May 18-21., 2008, Buenos Aires, Argetina. Circulation; e162-e413, 84, P468.

BARTHA E, MAGYAR K, SOLTI I, KERESKAI L, KALAI T, HALMOSI R, HIDEG K, SUMEGI B, TOTH K. Protective effect of a quinazoline-type poly(ADP-Ribose)polymerase inhibitor against the development of hypertensive cardiomyopathy and heart failure. Scientific Session 2008 of American Heart Association, November 8-12, 2008, New Orleans, USA, Circulation, 2008; 118:S_946, Abstract book 359.

RÁBAI M, PÁLFI A, BARTHA É, TÓTH A, MAGYAR K, SÜMEGI B, TÓTH K. Vörösbor és alkoholmentes vörösbor-kivonat protektív hatásai állatkísérletes és in vitro hemoreológiai modellekben. Magyar Kardiológusok Társasága 2009. évi Tudományos Kongresszusa, 2009. május 6-9., Balatonfüred, Card. Hung. Suppl. B, 2009; 39:A74.

BARTHA É, SOLTI I, KERESKAI L, PLÓZER E, MAGYAR K, LANTOS J, KÁLAI T, HIDEG K, SÜMEGI B, TÓTH K. A PARP-gátlás késlelteti a szívelégtelenség kialakulását spontán hipertenzív patkánymodellben. Magyar Kardiológusok Társasága 2009. évi Tudományos Kongresszusa, 2009. május 6-9., Balatonfüred, Card. Hung. Suppl. B, 2009; 39:A39.

BARTHA E, SOLTI I, KERESKAI L, PLOZER E, MAGYAR K, KALAI T, HIDEG K, SUMEGI B, TOTH K, HALMOSI R. Protective effect of a quinasoline-type poly(ADP-ribose)polymerase inhibitor against the development of hypertensive cardiopathy. Barcelona, Spain, Annual Congress of European Society of Cardiology, Aug 29- Sep 2., 2009, Barcelona, Spain. Abstract book 141.